creative commons
COMMONS DEED

저작자표시 2.0 대한민국

이용자는 아래의 조건을 따르는 경우에 한하여 자유롭게

- 이 저작물을 복제, 배포, 전송, 전시, 공연 및 방송할 수 있습니다.
- 이차적 저작물을 작성할 수 있습니다.
- 이 저작물을 영리 목적으로 이용할 수 있습니다.

다음과 같은 조건을 따라야 합니다:

저작자표시. 귀하는 원저작자를 표시하여야 합니다.

- 귀하는, 이 저작물의 재이용이나 배포의 경우, 이 저작물에 적용된 이용허락조건을 명확하게 나타내어야 합니다.
- 저작권자로부터 별도의 허가를 받으면 이러한 조건들은 적용되지 않습니다.

저작권법에 따른 이용자의 권리는 위의 내용에 의하여 영향을 받지 않습니다.

이것은 이용허락규약(Legal Code)을 이해하기 쉽게 요약한 것입니다.

Disclaimer

dCollection

Ph.D. DISSERTATION

Energy Management Techniques for Hybrid Energy Storage Systems in Electric Vehicles

전기차의 하이브리드 에너지 저장장치를 위한 에너지 관리 기법

2014 년 2 월

DEPARTMENT OF ELECTRICAL ENGINEERING AND
COMPUTER SCIENCE
COLLEGE OF ENGINEERING
SEOUL NATIONAL UNIVERSITY

Sangyoung Park

Energy Management Techniques for Hybrid Energy Storage Systems in Electric Vehicles

전기차의 하이브리드 에너지 저장장치를 위한 에너지 관리 기법

지도교수 장래혁

이 논문을 공학박사 학위논문으로 제출함

2013 년 12 월

서울대학교 대학원

전기·컴퓨터 공학부

박상용

박상용의 공학박사 학위논문을 인준함

2013 년 12 월

위 원 장	하순회	(인)
부위원장	장래혁	(인)
위 원	최기영	(인)
위 원	Samarjit Chakraborty	(인)
위 원	Massimo Poncino	(인)

Abstract

Electric vehicles (EV) are considered as a strong alternative of internal combustion engine vehicles expecting lower cost per mile, higher energy efficiency and low carbon emission. However, their actual benefits are not yet clearly verified while its energy storage system (ESS) can be improved in many ways. First, low cost per mile of EV is largely diminished if we charge EV with electricity from fossil fuel power plants due to power loss during generation, transmission, conversion and charging. On the other hand, regenerative braking is direct power conversion from the wheel to battery and one of the most important processes that can enhance energy efficiency of EV. Power loss during regenerative braking can be reduced by hybrid energy storage system (HESS) such that supercapacitors accept high power as batteries have small rate capability. Second, low cost per mile claimed by EV manufacturers does not take battery depreciation into account. Battery cost takes up to 50% of the total EV price, and its life is generally guaranteed for only 8~10 years. Harsh charge and discharge profiles of a battery results in reduced cycle life. Use of HESS and systematic charge management algorithms gives potential to mitigate the problems and improve various metrics of ESS such as cycle efficiency, cycle life, and so on.

This dissertation discusses design-time and run-time issues in HESS for EVs in order to maximize the energy efficiency and minimize the operating cost. This dissertation performs extensive optimization based on elaborate component models to achieve the objectives. First, we proposed systematic algorithms

to maximize the energy efficiency for a regenerative braking scenario, while most of the previous works relied on empirical and heuristic methods. We improve the energy efficiency by calculating the optimal charging power distribution between the supercapacitor bank and battery bank. Minimizing the cost per mile of an EV should consider optimization over a period of time including multiple acceleration and deceleration profiles. A little forecast on the future driving profiles helps prepare the supercapacitor state of charge (SOC) to the optimal level by systematic charge migration such that it can charge and discharge the electrical energy to enhance the energy efficiency. We also propose grid power source-aware EV charging technique to minimize the electricity bill from a home equipped with photovoltaic energy generation. Lastly, we implement an actual EV equipped with HESS to verify the proposed algorithms.

Keywords: Electric vehicle, Battery-supercapacitor hybrid, Regenerative braking, Charging/discharging asymmetry, Grid-connected photovoltaic System, Electricity bill minimization

Student Number: 2008-20881

Contents

List of Figures

List of Tables

Chapter 1

Introduction

1.1 Motivation for Electric Vehicle Energy Optimization

Electric vehicles (EV) are rapidly gaining popularity as demand for cleaner means of transportation increases. Most countries actively promote deployment of EV. Governments offer subsidies and tax credits to EV manufacturers and customers to give a boost to EV market. The US Government provides federal tax credits to EV consumers according to battery capacity of the vehicle such that Chevrolet Volt and Tesla vehicles are eligible for one-time $7,500 tax credit. The underlying assumption in this trend is that EV is more environmentally friendly and has lower cost per mile. However, their actual benefits, both economic and environmental, are not yet clearly verified while the energy efficiency can be improved in many ways.

Cost per mile of a FEV Nissan Leaf is just 3.5 cents assuming 11 cents/kWh

Table 1.1 Claimed cost benefits of EV and battery depreciation.

Vehicle	Vehicle price	Cost per mile	Battery depreciation ($/mile)
Nissan Leaf	$35,430	$0.035	$0.102
Chevy Volt	$43,700	$0.038	$0.068
Tesla Model S (60 kWh)	$95,800	$0.042	$0.257
Toyota Prius	$32,000	$0.086	$0.019

electricity [23] while conventional petroleum cars requires about 15 cents for a mile. High battery depreciation results from high initial cost of the high capacity batteries and its relatively short lifetime. The portion of battery cost in initial vehicle price is often up to half of the total price. The ever best selling FEV Nissan Leaf's price without any subsidies in US is $35,430, where Nissan Leaf battery cost is close to $18,000 [48]. Nissan Leaf battery warranty is for 160,000 km or eight years. A brief calculation of based on approximate battery cost of $500/kWh gives cost per mile to be over 10 cents, which is significantly higher than the claimed cost per mile. The vehicle cost, cost per mile, and battery depreciation of representative EVs are shown in Table 1.1. A recent analysis points out that the maximum annual profit considering the real power grid electricity price and battery degradation is only $10 to $120 per EV, which is definitely not sufficient to attract the customers due to the higher EV price comparing with internal combustion engine vehicle [44].

Moreover, the cost per mile calculation and cleanness of EVs should be evaluated considering the grid side. The energy efficiency from chemical energy stored in fossil fuel to actual traction energy should not be dramatically different from petroleum-powered vehicles. For example, average power plant boiler and turbine efficiency is at around 33% [5], power transmission efficiency is at around 93%, battery charger shows at around 90% efficiency [24], and the battery

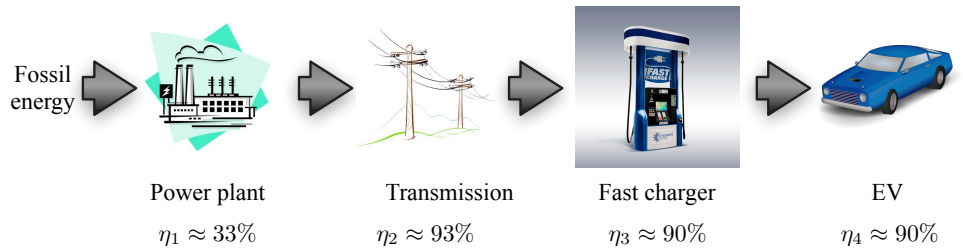

Figure 1.1 EV energy efficiency considering grid power generation and transmission.

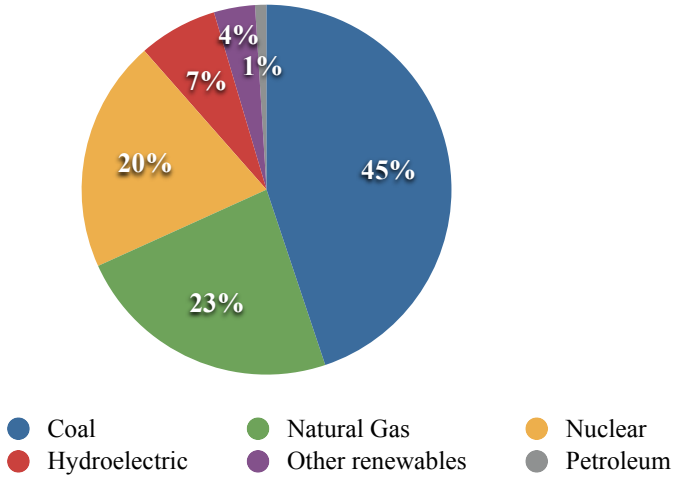

Figure 1.2 2009 US electricity generation by source.

charging efficiency is at around 90% [10, 60] as shown in Figure 1.1. The overall efficiency is at around 25%, which is not meaningfully higher than the efficiency of internal combustion engines, which is known as 25~30%.

This also means that the environmental impacts might not be so low as they are widely advertised. The carbon emission of the overall energy chain for using EVs is dependent on the source of grid electricity. For example, carbon emission of Mitsubishi iMiEV in San Francisco is 100 g/mi, while in Denver, it

is 290 g/mi [21]. This is because the source of grid electricity is cleaner in San Francisco. The source of grid electricity is an important factor in evaluating carbon emission because current electricity grids rely largely on fossil fuel as shown in Figure 1.2. The carbon emission benefits from EV is largely diminished if we charge EV with electricity from coal power plants due to power loss during generation, transmission, conversion and charging. A traditional coal plant efficiency is 30~35% [5], power transmission efficiency is at around 93%, battery charger shows at around 90% efficiency, and the battery charging efficiency is at around 90% [10, 60]. The overall efficiency is at around 26%, which is not meaningfully higher than the efficiency of internal combustion engines, which is known as 25~30%.

The listed facts motivate the need for improving the efficiency of ESS for EVs and charge management to maximize the user benefits. It is dangerous to simply assume that EVs provide lower cost per mile and carbon emission. We need to carefully evaluate the benefits of EVs to correctly design the ESS and perform charge management.

1.2 Research Contributions

The main contribution of this dissertation is system-level view of energy efficiency and operating cost optimization of EVs, while prior works have largely relied on expert rules, heuristics or tedious learning-based algorithms, which prohibited efficient search of the global optimum. More specifically, this dissertation aims at improving the energy efficiency of ESS in EVs mainly focusing on optimized runtime charge management in HESS. I also review the cost of ownership of EVs from the perspective of EV charging cost reduction of resi-

dential photovoltaic systems. Our approach precisely defines the optimization objectives, constraints and derives solution algorithms based on well-defined component models.

System-level charge management and optimization algorithms relies on component models for efficient design space exploration and accurate solutions. Thus, this dissertation first covers the models of the components that comprise EV powertrain in the background section. Many of the component models have been well-studied in prior context. However, selecting the model with appropriate level of abstraction is crucial for trading-off solution quality and easiness of solution space exploration. This dissertation reviews the component models from the system-optimization perspective and choose simple analytical component models.

This dissertation solves three optimization subproblems, which emphasizes system-level approaches to improve the energy efficiency and cost of ownership of EVs. The first problem is maximum power transfer tracking (MPTT) of regenerative braking energy. The problem addresses the importance of conditioning the peripheral electric circuits, that is, DC–DC converters and chargers, and charging currents for each energy storage elements in transferring the maximum amount of energy from the motors to ESS during regenerative braking. The concept of this problem is adopted from maximum power point tracking (MPPT) of solar-cell powered systems, which require elaborate conditions of the operating points due to non-idealities in the power source. We show that component efficiency models we use actually matters in overall system efficiency.

The second problem represents a broader view of the HESS charge management, while the first problem addresses the importance of elaborate component

models' effect on energy efficiency. SOC management of supercapacitor-battery HESS over a driving cycle leads to energy efficiency improvement in a longer term. This statement does not negate the conclusions of the first problem, but provides a wider view of optimization. That is, the component models used in the first problem will also be used in systematic optimization of the HESS charge management problem in a longer timer period. We show that the prediction of the future driving patterns and performing proactive charge management improves the energy efficiency.

The third problem addresses yet a different perspective, which is the cost of EV charging. The portion of EVs in current car market is not yet very significant, which allows the electricity utility companies to provide EV charging power at a low cost. However, this situation will change substantially if the government and companies succeed in attracting customers to purchase EVs up to a significant portion of the total vehicle market. As we will discuss in Section 2, the carbon emission and global energy efficiency depends on the source of grid electricity. It is desirable to use non-fossil fuel generated power such as renewable energy. We assume a number of residential EV charging scenarios equipped with photovoltaic (PV) array installations. We devise a method to achieve the minimum electricity bill for supplying the residential load and EV charging.

The contributions are summarized as follows.

- Improve energy efficiency of EV ESS by hybrid usage of energy storage elements
- Characterization of EV components, which can be leveraged for system-level design space exploration

- Address importance of maximum power point tracking (MPPT) and efficiency of conversion circuitry in energy efficiency
- Address necessity and potential of improving energy efficiency for long-term charge management of HESS in EVs
- EV prototype implementation for evaluation of HESS

1.3 Thesis Organization

Chapter 2 discusses the background and related work on EV component modeling, ESS design, and basic operating principles. Chapter 3 addresses the importance of power conversion efficiency in regenerative braking and devises a maximum power transfer tracking algorithm. Chapter 4 describes the charge management problem and introduces supercapacitor hybrid ESS to enhance the overall energy efficiency and regenerative braking efficiency. Chapter 5 discusses EV charging in grid-connected solar power systems to minimize the electricity bill. Chapter 7 concludes this dissertation and discusses the future work including implementation of EV prototype.

Chapter 2

Background and Related Works

2.1 Electric Vehicle Powertrain Generals

Powertrain of FEVs and HEVs: An EV powertrain is a group of components that generate power and deliver it to the road surface. The general architectures of FEVs and HEVs are shown in Figure 2.1. A FEV powertrain comprises an energy storage, a charger, a DC–DC converter, an inverter/rectifier, a motor, and a transmission as shown in Figure 2.1(a). A HEV can be roughly categorized into parallel HEVs and series HEVs as shown in Figures 2.1(b) and (c). A parallel HEV contains ICE and differential gear to mix the traction power from the ICE and motor. A series HEV contains ICE only for charging the energy storage via electric generator. The traction power is solely supplied by the motor.

Energy storage system: The energy storage system in an EV stores electrical energy and provides traction power during driving, and receives regener-

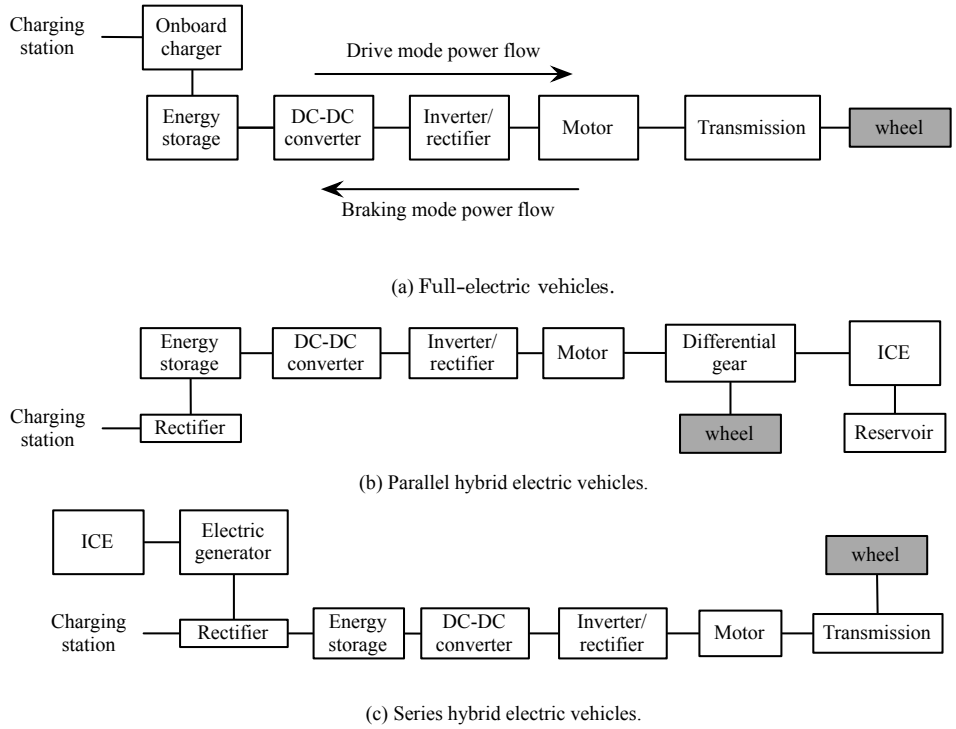

Figure 2.1 Electric vehicle powertrain architecture.

ative energy during braking. Energy storage in EVs is different from starting, lighting, and ignition (SLI) batteries in traditional petroleum-powered vehicles in that it should be able to supply traction power over a certain period of time. Energy storage in EVs require high power capacity and high energy density. Lead-acid batteries used in conventional non-EVs is generally not considered appropriate as the energy storage in EVs because it cannot satisfy the requirements.

The type and capacity of energy storage of commercial FEVs and HEVs are shown in Table 2.1. Commercially available FEVs and HEVs mostly rely on Li-ion battery technology, while some models use NiMH batteries. All of them

Table 2.1 Energy storage used in various EVs.

Vehicle	Type	Energy storage		Range (km, EPA drive cycle)
		Type	Capacity	
Nissan Leaf	FEV	Li-ion	24 kWh	135
Chevy Volt	Extended range EV	Li-ion	16.5 kWh	61 (electric), 610 (extended)
Mitsubishi iMiEV	FEV	Li-ion	16 kWh	100
Tesla Model S	FEV	Li-ion	85 kWh	426
Toyota Prius	HEV	Li-ion	4.4 kWh	18 (electric), 870 (full)
Honda Insight	HEV	NiMH	0.58 kWh	N/A

(a) Chevy Volt battery system (16.5 kWh, Li-ion)

(b) Nissan Leaf battery system (24 kWh, Li-ion)

Figure 2.2 Battery system in commercial EVs.

are homogeneous battery bank, which is an array of modules again containing a number of cells. Despite the recent advance of battery technology, the energy density of the batteries is still orders of magnitude smaller than that of petroleum. This becomes a huge limiting factor in extending drive range of EVs.

Motor: Motors provide traction power to drive the vehicle. Motors convert electrical power to mechanical power during drive mode. Motors can generate electricity and converts mechanical power to electrical energy during re-

Table 2.2 Motors used in various EVs.

Vehicle	Type	Motor type	Power (kW)	Torque (N·m)
Nissan Leaf	FEV	PM	80	280
Chevy Volt	Extended range EV	PM	111	370
Mitsubishi iMiEV	FEV	PM	47	180
Tesla Model S	FEV	AC induction	310	600
Toyota Prius	HEV	PM	60	N/A
Honda Insight	HEV	NiMH	9.7	79

generative braking mode. The two most popular types of motors used in EV are 3-phase permanent magnet synchronous motors (PMSM) and 3-phase AC induction motor. Most of the compact and mid-size passenger vehicles equip 3-phase PMSM. PMSMs are synchronous AC motor or brush-less DC motor (BLDC) motor. The output power of a PMSM is limited by the size of the permanent magnet [66]. Parallel HEVs does not require a high-power motor, thus, not requiring a large, expensive permanent magnet. This makes PMSMs suitable for parallel HEV applications such as Toyota Prius and Honda Insight or compact cars such as Nissan Leaf and Mitsubishi iMiEV [9]. High-performance EVs like Tesla Model S require very high motor output power. AC induction motors are used for this type of vehicle.

Power conditioning, management, and control components: EV powertrain contain power conditioning, management, and control circuits such as DC–DC converter, onboard charger, and inverter/rectifier. They control the electrical power flow in the powertrain. The inverter provides 3-phase AC power to drive the motor. The inverter is a 3-phase bridge circuitry controlled by pulse width modulated (PWM) signals. The inverter also works as a rectifier during regenerative braking. As the DC bus voltage of the EVs well exceed

a few hundred volts, IGBTs are considered better option than MOSFETs for implementing the switches in the driver.

A DC–DC converter is also required to condition and control the DC bus voltage. DC–DC converters minimize the fluctuations in the DC bus voltage due to battery state-of-charge (SOC) change, open circuit voltage (OCV) variations, which leads to motor performance degradation. A DC–DC converter is also essential for stable regenerative braking. For example, an abrupt change in DC bus voltage occurs during transition from motoring to regenerative braking [8]. A DC–DC converter maintains constant voltage in the DC bus voltage and prevents damage in the batteries and degradation of the motor.

Transmission: Most EVs use single-speed fixed ratio transmission. The efficiency of the motor is relatively constant over a wide range of RPM compared with the internal combustion engines (ICE), which makes single-speed transmission viable for use in EVs. Some research works consider two-speed transmission for EVs [19]. However, all the commercially available vehicles use single-speed transmission.

It is essential to understand the operation of components in the powertrain and model its efficiency to perform systematic optimization. Study on motor drivers, DC–DC converters and motors is a classical topic, and there has been extensive amount of work in modeling and characterization of the components in EV powertrain [56, 62, 65, 66, 32, 20]. However, it is important to identify important parameters and extract abstracted models with reasonable complexity and accuracy to be used in systematic optimization.

2.2 Electric Vehicle Powertrain Modeling

2.2.1 Vehicle Modeling

The energy efficiency of the EV power train depends on efficiency of its consisting components starting from the traction force on the wheels to axle, motor, inverter, charger, and finally, to ESS banks. Speed and traction force of the vehicle is converted to motor torque and rpm by the following steps. Traction force is equal to total running resistance which is described as,

$$R_{tot} = R_R + R_A + R_G + R_I + R_B, \tag{2.1}$$

where R_R, R_A, R_G, R_I, and R_B are rolling resistance, aerodynamic resistance, gradient resistance, inertia resistance, and brake force provided by hydraulic brakes, respectively. Simple models exists for calculating the resistance values using vehicle mass, drag coefficients, drag area, vehicle speed, and so on [67].

$$R_R = C_{rr}W, \tag{2.2}$$

$$R_A = \frac{1}{2}\rho C_d A v^2, \tag{2.3}$$

$$R_G = W sin\theta, \tag{2.4}$$

$$R_I = ma, \tag{2.5}$$

where C_{rr}, W, C_d, A, v, θ, m, and a is the rolling resistance coefficient, vehicle weight, air density, drag coefficient, car frontal area, vehicle speed, gradient angle, vehicle mass, and vehicle acceleration, respectively. We calculate the motor torque and angular velocity from the traction force, wheel size and axle ratio

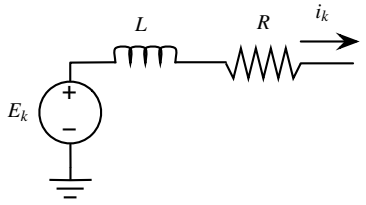

Figure 2.3 BLDC equivalent circuit model per phase.

information. Many EV have single speed constant ratio transmission, which makes the calculation the easier.

$$R_{tot} - R_B = \tau_w d_w / 2, \tag{2.6}$$

$$\tau_m = \tau_w / G, \tag{2.7}$$

$$\omega_m = \frac{v}{\pi d_w} \cdot 2\pi = \frac{2v}{d_w} G, \tag{2.8}$$

where $F_{traction}$, τ_w, τ_m, G, ω_m, d_w are traction force, wheel torque, motor torque, axle ratio, motor angular velocity, and wheel diameter.

2.2.2 Motor and Control Circuitry

Motor: Motors used in EVs are generally a permanent magnet synchronous motor (BLDC) or AC induction motor. A BLDC motor is often modeled by the equivalent circuit given in Figure 2.3.

$$V_k = Ri_k + (L - M)\frac{di_k}{dt} + E_k, \tag{2.9}$$

$$E_k = K_k \omega_m F(\theta_e + \theta_k), \tag{2.10}$$

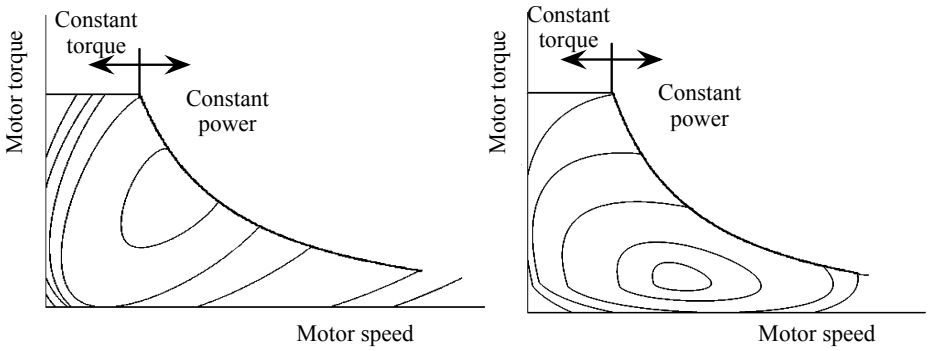

(a) Typical efficiency map of a PMSM. (b) Typical efficiency map of a induction motor.

Figure 2.4 Typical efficiency map of motors according to torque and speed [66].

$$T_k = K_t i_k F(\theta_e), \tag{2.11}$$

where V_k, E_k, T_k, i_k are the voltage, back-electromotive force (EMF) voltage, torque, and current of k-th phase, R, L are the resistance, inductance of each phase, M is the mutual inductance, K_t and K_e are the torque constant and back-EMF constant, ω_m and θ_e are the angular speed and angle of the rotor, $F(\theta_e)$ is the back-EMF reference as function of rotor, θ_k is the phase difference between phases [57]. Back-EMF voltage is proportional to the

The motor efficiency is defined as the ratio of input electrical power to the output mechanical power.

$$\eta_{motor} = \frac{P_m}{P_e}, \tag{2.12}$$

where P_m and P_e are output mechanical power and input electrical power, respectively.

$$P_e = \sqrt{3} V_{rms} \cdot I_{rms}, \tag{2.13}$$

$$P_m = \tau \cdot \omega, \tag{2.14}$$

where V_{rms}, I_{rms}, τ and ω are RMS voltage between the two phases, RMS current of a phase, motor torque and angular velocity, respectively. The term $\sqrt{3}$ is for delta internal connection in the 3-phase motor. Typical efficiency maps of a 3-phase BLDC motor and AC induction motor is given in Figure 2.4. A motor is usually operated at constant torque in low motor speed region and at constant power beyond the region. Motor power loss consists of copper loss in stator/rotor, core loss, friction and windage loss, and stray loss. A general equation on motor loss is given as,

$$P = I_a^2 R_a + I_f^2 R_f + K_i B_g^2 N^2 + K_m N^3 + K_{st} I_a^2 N^2, \tag{2.15}$$

where the each product term means armature copper loss, field copper loss, core loss, frictional loss, and stray loss, respectively. The copper losses are ohmic loss in the stator and rotor windings expressed in I^R form. The core loss is the loss due to magnetization of the core material. It consists of hysteresis loss and eddy current loss. The amount of loss is proportional to square of rotational speed of the motor and the strength of magnetic flux. Friction loss is due to mechanical friction in the motors. Stray loss is includes all losses, which are not accurately determinable. It is usually regarded a function of both load current and motor rotational speed.

Motor driver: A motor driver is generally IGBT-based 3-phase bridge circuitry as shown in Figure 2.5. IGBT-based drivers are superior to MOSFET-based drivers in EV traction system because it utilizes DC voltage of several hundred volts and current of a few hundred amperes. Power loss in the motor

Table 2.3 Sources of motor losses [59].

Friction and windage	5%–15%
Core (iron) losses	15%–25%
Stator (I^2R)	25%–40%
Rotor (I^2R)	15%–25%
Stray load	10%–20%

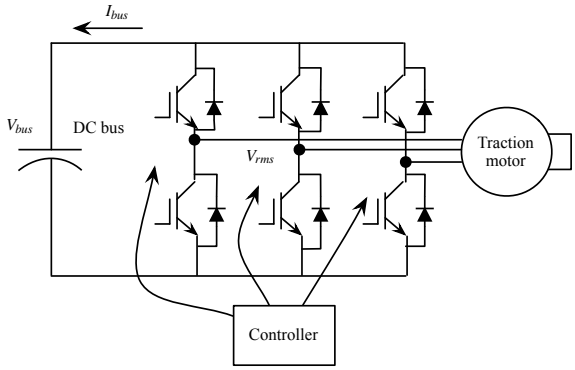

Figure 2.5 3-phase IGBT-based motor driver.

driver consists of conduction loss, switching loss, and diode loss just like the DC–DC converter loss for electronics loads.

$$P_{loss} = P_{cond} + P_{sw} + P_d \tag{2.16}$$

Conduction loss: The conduction loss of a IGBT depends on collector to emitter saturation voltage as shown in (2.17). This is different from MOSFET-based converters where the conduction loss depends on the on resistance.

$$P_{cond} = V_{CESAT} \cdot I_{RMS}, \tag{2.17}$$

The portion of V_{CESAT} is negligible if the DC bus voltage becomes well over a few hundred volts. This will result in lower conduction loss than MOSFET-based converters in EV applications.

Switching loss: The switching loss depends on IGBT turn on energy, E_{on}, turn off energy E_{off} and base switching frequency f_{sw} as shown in (2.18).

$$P_{sw} = (E_{on} + E_{off}) \cdot f_{sw}. \tag{2.18}$$

The detailed calculation of E_{on} and E_{off} requires some math [46], but it is not very difficult to calculate. The value of E_{on} and E_{off} depends on various device parameters such as rise time, fall time, etc.

Diode loss: The diode loss occurs during IGBT off-time due to reverse recovery in the freewheeling diode. Even the modern fast recovery diodes still

consume a noticeable amount of power.

$$P_d = f_{sw} \int_0^{t_{rr}} V_d I_d dT. \tag{2.19}$$

DC–DC converter: DC–DC converter efficiency is a strong function of input voltage, output voltage and load current. The power loss is classified into conduction loss, switching loss and controller loss.

$$P_{dcdc} = P_{cond} + P_{sw} + P_{ctrl}. \tag{2.20}$$

There have been well studied models on the efficiency of DC–DC converters [15]. In general, we can perform curve-fitting with input voltage, output voltage and load current of a DC–DC converter to model the efficiency plane [33]. Conversion efficiency of inverters and chargers in EV power train is not constant. We describe them as a function of V_{in}, V_{out}, I_{out}, which are input voltage, output voltage and output current with reasonable accuracy [15]:

$$\eta = f(V_{in}, V_{out}, I_{out}). \tag{2.21}$$

2.2.3 Energy Storage Elements

Battery is the key component, which is related to most of the performance metrics of an EV. Electrochemical models of batteries have been developed [50, 47]. However, they are too complex to be used in systematic optimization. One of the most important aspect of battery efficiency loss is the rate capability [54].

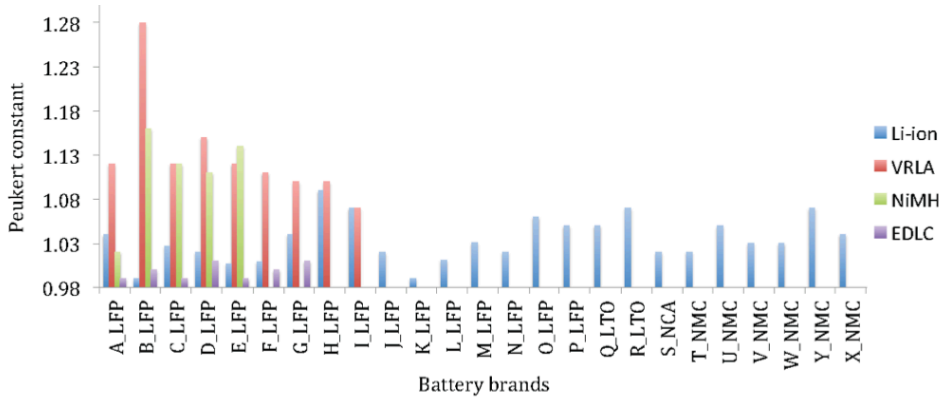

Figure 2.6 Peukert's constant of various types of batteries [39].

Rate capability is usually explained by the Peukert's law.

$$C_p = I^k t, \tag{2.22}$$

where C_p is the battery capacity at a nominal discharge current in Ampere-hour, I is the battery current relative to the nominal battery current, k is the Peukert's constant and t is time in hours.

Figure 2.7(a) illustrates the rate capability of a Li-ion battery by the discharging current ranging from 1C to 6C. A higher C-rating current significantly decreases the amount usable energy extracted from the battery [55]. We observe the same phenomena for the charging operation.

Peukert's constant k of various technology values is shown in Figure 2.6. Due to the advance of Li-ion battery technologies, the Peukert's constant for the state-of-the-art models is assumed to be smaller than 1.05. The battery cycle efficiency has been greatly improved in recent years. However, battery cycle efficiency problem at high loads still remain. A recent study shows that

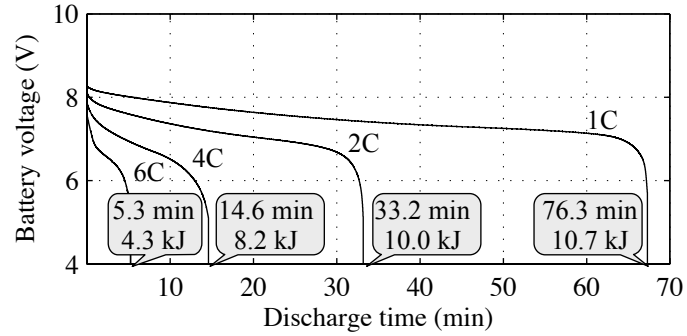

(a) Rate capability [18].

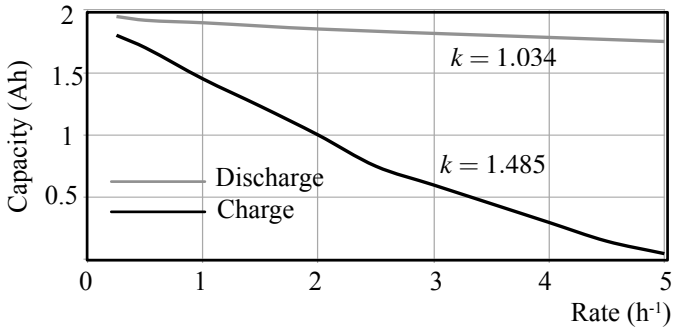

(b) Peukert plot of a 1.9 Ah 18650 Li-ion cell [5].

Figure 2.7 Battery characteristics.

Table 2.4 Energy densities of common energy storage materials.

Storage material	Energy type	Energy density (MJ/kg)
Gasoline	Chemical	~46
LPG	Chemical	46.4
Lithium-ion battery	Electrochemical	0.72~0.875
Nickel-metal hydride battery	Electrochemical	0.288
Lead-acid battery	Electrochemical	0.17
Supercapacitor	Electrical	0.018
Electrostatic capacitor	Electrical	0.000036

the battery current often goes up to 4 C during rapid acceleration [49]. A simple calculation of efficiency loss with a battery having 1.05 Peukert's constant value during 4 C charging is $\frac{4}{4^{1.05}} = 93\%$. Lower efficiency during charging also becomes problematic in case of quick charging. Most of the EVs support quick charging, which finishes charging by 15~30 minutes, which is equivalent to 2~4 C current [28]. Degraded efficiency not only causes heating problems, but also brings up cost per mile issue.

Supercapacitor Supercapacitors, on the other hand, does not suffer from efficiency degradation during high current charging and discharging. The cycle efficiency is virtually 100%. However, the energy density of supercapacitors is 0.018 MJ/kg, while that of Li-ion batteries is 0.72~0.875. This makes the supercapacitor not suitable for main energy reservoir for EVs. Thus, many works focus on using supercapacitor as a temporary energy storage capable of handling only one time braking and acceleration [12, 40, 52, 11].

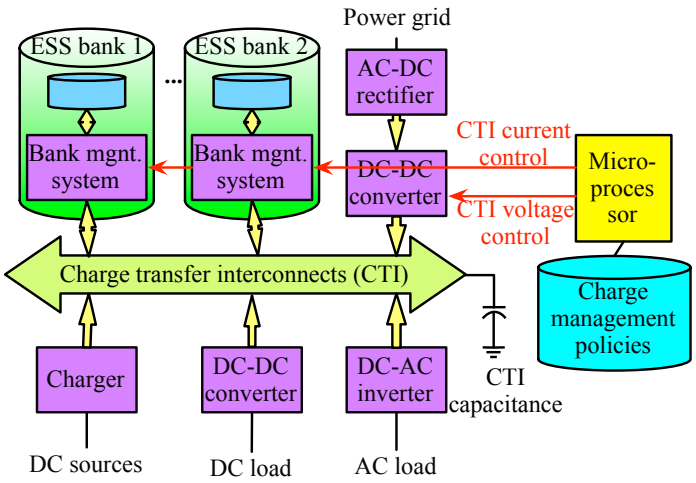

Figure 2.8 HESS architecture [43].

2.3 Hybrid Energy Storage System

2.3.1 Architecture

General HESS architecture has high degree of freedom, which allows many heterogeneous types of energy storage elements and connection topology as shown in Figure 2.8 [43, 29]. A HESS comprises ESS banks, bank management systems (BMS), charge transfer interconnects (CTI), DC–DC converters, DC–AC inverters, power sources, load devices, and a microprocessor-based charge management policy controller. An ESS bank typically consists of homogenous ESS elements organized into a two-dimensional array to meet the power/energy capacity and the voltage rating. There is also a bidirectional charger (or two unidirectional chargers connected in opposite directions) that controls the charge and discharge current of the ESS array (or equivalently, the current flowing into and out of the ESS bank.) Because the SoC, terminal output voltage, and power rating of different ESS arrays may not be compatible with each other,

direct connection among ESS arrays is generally not feasible. A BMS controls charging and discharging currents of the relevant ESS bank and performs basic conditioning functions such as cell balancing and protection. A CTI becomes the path for transferring charge to/from/among the grid/load/ESS banks. The primary function of CTI is to provide charge transfer paths among storage banks, power sources and load devices. There are various ways to implement CTI including a single DC bus wire, a segmented DC bus, multiple DC buses, or a more complicated interconnect network such as a mesh network [43, 29]. Converters for the power sources and load devices can be any of chargers, DC-DC converters, AC-DC rectifiers, and DC-AC inverters as appropriate. These components are not different from the components in a homogeneous ESS system. Charge management policy controller is a microprocessor-based controller in charge of the CTI current flowing from or to each ESS bank and the CTI voltage according to the elaborated charge management policies.

A combination of a battery and an energy storage element with a higher power capacity can be a good complementary setup both for efficiency and cost in ESS for regenerative braking. Among them, battery-supercapacitor HESS is considered a promising solution to mitigate rate capability problem of batteries while meeting other ESS constraints. Adding appropriate amount of supercapacitor could increase the overall energy efficiency and thus the cruise range. Despite its benefits, supercapacitor is still expensive and cause severe volumetric overhead in EV. Therefore, the key issue in HESS is determination of the supercapacitor capacitance and SoC management.

2.3.2 HESS Management

Charge management of HESS is categorized into three operations, which are charge allocation, migration and replacement. The terms are analogous to the terms used in cache management in computer architecture. Charge is managed just as the cache data is managed. Charge allocation determines (i) destination EES banks to be charged from a power source, (ii) the amounts of charging current of destination banks and (iii) the CTI voltage. The goal of the charge allocation problem is to maximize the charge allocation efficiency of the system. Charge replacement (discharging the HESS to the load device or the power grid) selects one or more source EES banks and also determines the amounts of discharging current of the source EES banks for a given load. The goal of the charge replacement problem is to maximize the charge replacement. Charge migration exchanges charge among various ESS banks. The charge migration is a unique feature in the HESS that is not necessary in a homogeneous ESS system. The optimal ESS banks for charge allocation and for charge replacement can be different in general. Some ESS banks are not suitable for long-term energy storage due to large self-discharge rate despite their high efficiency for charge allocation and/or charge replacement such as a supercapacitor bank [43]. However, charge migration is an expensive process due to energy loss, and thus need to be carefully used.

Charge management such as charge allocation, replacement, and migration requires careful determination of sources, destinations, amount of current, CTI voltage, and so on, in order to maximize the energy efficiency, which is defined as

$$\eta_{transfer} = \frac{\text{Total energy transferred to the destination}}{\text{Total energy extracted from the sources}}, \tag{2.23}$$

where the sources are power sources or discharging ESS banks, and the destinations or load devices or charging ESS banks. According to the observation from recent related works [69, 63, 68, 64], charging efficiency is strongly dependent on the type of the bank, the magnitudes of the charging currents, SoCs of the EES banks, voltage and current characteristics of the external power source, and so on. Excessive mismatch between the input voltage level and the EES bank terminal voltage results in unnecessarily large power loss in the chargers. Severe mismatch between the input current and the destination EES bank charging current results in a high IR loss and rate capacity effect. The destination EES banks must be compatible with the input power source in terms of the energy capacity as well.

2.3.3 HESS Management for EV

A heuristic approach can maintain the supercapacitor SoC inversely proportional to the vehicle speed [12], and use of machine learning to avoid modeling complexity of the entire regenerative braking process [40]. Such complicated problems are often solved by intuitive methods based on expert rules. This type of heuristic approach enhance load balancing among the fuel cell, battery, and supercapacitor [52]. Cost of power converter is additional overhead for the SoC management of supercapacitor, and sometimes, size of the power converter has a higher priority over energy efficiency in the supercapacitor SoC management [11]. Such SoC maintenance significantly restricts the efficient charging and discharging during acceleration and braking [13].

Previous works mostly focused on supercapacitor SoC so that supercapacitors are not fully charged during regenerative barking and not fully depleted

during acceleration. Unfortunately, optimization of the HESS charging efficiency is not accordance with the ideal supercapacitor SoC management [13]. Therefore, SoC management of the supercapacitor generally override the efficiency optimization.

2.4 Electric Vehicle Charging

EV charging infrastructure from a global point of view has also caught attention of the researchers. A comprehensive study evaluates various infrastructure scenarios of charging such as i) overnight charging at home garage, ii) overnight charging at apartment complex, iii) opportunity charging at commercial facility, and charging standards, which differs in charging voltage and current [38]. There are multiple objectives when considering co-optimization of electric vehicle charging with the grid such as minimizing power loss, reducing charging time, minimizing the daily electricity cost, and stability of the grid, etc. The impact of EV charging load demand would become significant on the grid stability when number of deployed EVs increase. A recent work has estimated that 35.8% increase in peak load for the worst case scenario [45]. Coordinated charging using stochastic quadratic and dynamic programming is proposed minimize power losses [16]. Another dynamic programming scheme was proposed to minimize daily electricity cost while suppressing battery degradation under certain limits [51]. A charging algorithm at global scope reduces peak power by 4% compared with local charging algorithm [37]. The impact of DC fast charging stations on future smart grids have been also investigated [6]. Another work considers various types of clean means of transportation and finds out, which combination minimizes the carbon emission [58].

Chapter 3

Maximum Power Transfer Tracking for Regenerative Braking

3.1 Regenerative Braking of Electric Vehicles

Regenerative braking is the key feature in EV to enhance energy efficiency as it allows reuse of kinetic energy during braking. It is widely adopted in commercial EV and HEV including Toyota Prius, Honda Insight, Tesla Roadster, and Chevrolet Volt. Figure 3.1(a) shows a typical regenerative braking system. Regenerative brakes in EV involve using an electric motor as an electric generator and stores energy in energy storage for later use. Not all of the kinetic energy is recovered using regenerative braking due to the following reasons. Regenerative brakes alone cannot make the vehicle to a complete stop, and it only works on wheels with an electric motor, whereas braking force is often required from other wheels. Figure 3.1(b) shows a typical braking pattern. Regenerative braking force plus hydraulic braking force should match the driver

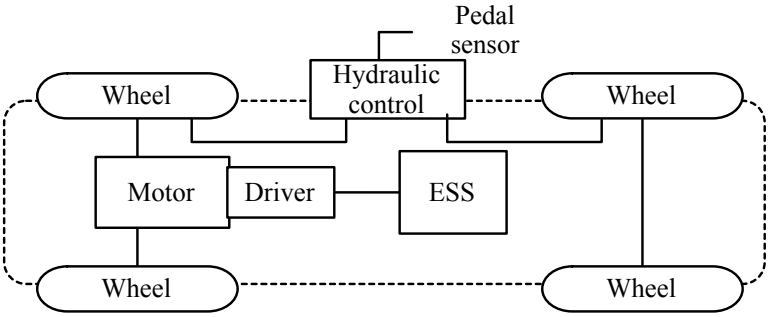

(a) A regenerative braking system.

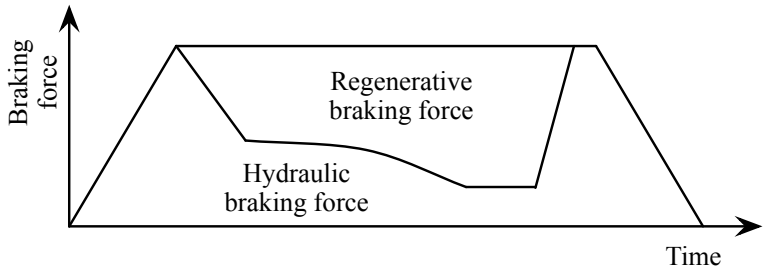

(b) A typical regenerative braking pattern.

Figure 3.1 Regenerative braking for EV.

demand from pedal sensor. In this chapter, we do not control the portion of regenerative braking force and hydraulic braking force, and thus we assume there is a well-defined control algorithm that maximizes regenerative braking energy while meeting the driver's demands. Thus, hydraulic brakes should always be used together with regenerative brakes, so some portion of kinetic energy will still be dissipated as heat. However, the portion of regenerative braking force to the hydraulic braking force is not very controllable because it should satisfy the driver's demands and match pressure on the pedal sensor.

Braking energy is often above 30% of traction energy and goes up to 80% in heavy city traffic [70]. Regenerative braking is effective battery recharging with the energy directly coming from the wheels to the battery unlike the long

lossy energy trip from the power plants for plugin recharging. Thus, efficient harvesting of regenerative braking energy is the key to maximize the annual profit of EV ownership. A brief calculation shows that increasing the regenerative braking efficiency by 10% is equivalent to 3% to 8% of improvement in the gas mileage.

3.2 Battery-Supercapacitor HESS Benefits

As the cruising range is one of the most important metrics of electric vehicles (EVs), the efficiency of the energy storage is crucial. It is well known that batteries are subject to the *rate-capacity effect* such that a larger charging/discharging current results in less amount of usable battery energy. The maximum charging current of most secondary batteries is much smaller than their maximum discharging current, and so the rate-capacity effect is said to be more serious for charging operations. Therefore, power capacity of batteries is often short during the charging process while driving, that is, regenerative braking for EVs. Supercapacitors, however, have a very high power capacity both for the charging and discharging operations and are not subject to the rate-capacity effect. Such characteristics of supercapacitors have inspired battery and supercapacitor *hybrid storages*, shown in Figure 3.2 [36, 40, 12], for EVs. There are two goals to achieve in the hybrid storage: maintaining a stable state of charge (SoC) of the supercapacitors and achieving high energy efficiency of the hybrid storage. As supercapacitors have relatively much smaller energy capacity in comparison with batteries in a typical hybrid storage, previous works mostly focused on supercapacitor SoC management [36, 40, 12].

Recent hybrid storages perform active SoC control of the supercapacitors

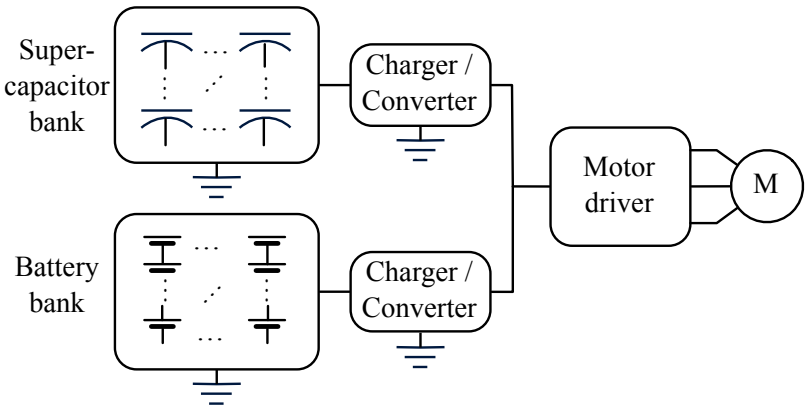

Figure 3.2 The topology of target electric vehicle energy storage.

using a charger. The charger efficiency should be carefully considered because it is largely variable by the supercapacitor SoC and the magnitude of the charging current [30]. These make it even more difficult to determine when and how to charge/discharge the supercapacitor and battery banks. This section introduces a method that deals with these two important considerations, which have not been thoroughly studied yet.

3.3 Electric Vehicle HESS SOC Management

Since supercapacitors have cycle efficiency advantage over batteries, charging the supercapacitor bank as much as possible and later charging the batteries may result in a higher energy efficiency [12]. Speed-sensitive charge management of supercapacitors may enhance the efficiency of the hybrid storage system [40]. When the vehicle speed is low, there are higher chances of acceleration which requires high-power discharging, and thus a high supercapacitor SoC helps. When the vehicle speed is low, there are higher chances of regenerative braking, which

generates high power from the traction motor, and thus low supercapacitor SoC helps. It is beneficial to limit the current flow to and from the batteries and to handle excess current with the supercapacitors, since it mitigates the rate-capacity effect of the batteries [36].

However, most of the previous works does not seriously consider one important factor: the power converter efficiency and the maximum power transfer from the traction motor during regenerative braking. In this chapter, we jointly consider the efficiency of both the batteries and supercapacitors, and the converter efficiency so that the maximum power can be transferred from the traction motor to the hybrid storage.

3.4 Maximum Power Transfer Tracking for Regenerative Braking

3.4.1 Concept of Maximum Power Transfer Tracking

We aim at EV power optimization from the perspective of HESS optimization [43]. The cycle efficiency of an HESS system is determined by the cycle efficiency of the storage elements and the power conversion efficiency of the power conversion circuits. In addition, it is important to maximize the actual power delivered from the power source to the hybrid [30].

The concept of MPTT has first been introduced PV-supercapacitor energy harvesting system [30]. A PV cell is susceptible to changes in the surrounding environment, which includes solar irradiance and operating temperature. This characteristic of a PV cell requires MPPT technique to maintain reasonable operating range to maximize its output power. A recent work has figured out that not only the PV output power, but also DC–DC converter efficiency plays

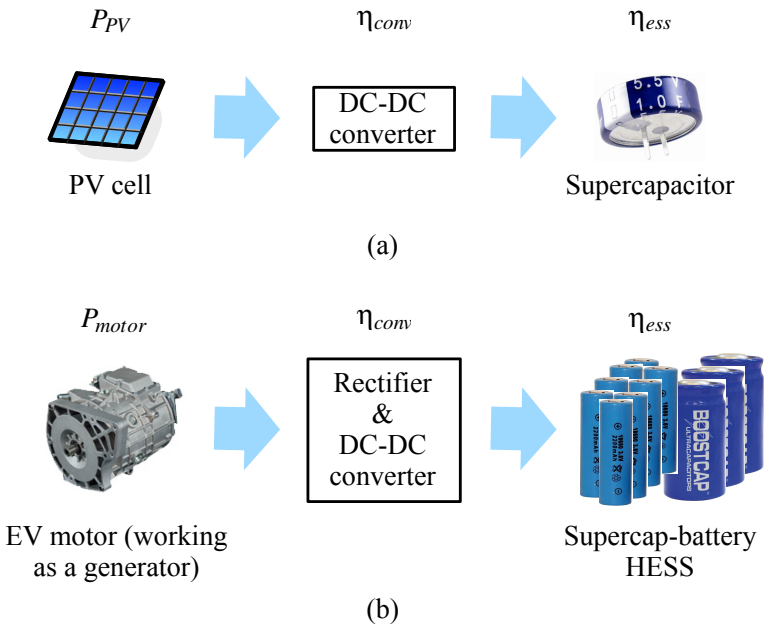

Figure 3.3 The concept of MPTT for (a) PV system [30], and (b) EV regenerative braking.

an important role in overall system energy efficiency [30]. A DC–DC converter efficiency is usually a function of input voltage, output voltage and output current as discussed in Section 2.2.2.

Motor power generation during regenerative braking is a direct function of torque and RPM of the motor, which are again dependent on the braking profile. Equation (2.11) indicates that the output voltage of a motor could vary from zero (when stopping) to the voltage close to the battery closed circuit voltage. We thus need a wide input voltage range DC–DC converter to maximize the regenerative braking energy utilization. However, the efficiency of the DC–DC converter degrades significantly if the voltage difference between the input and output side differs a lot. Thus, we adopt the concept of MPTT from PV supercapacitor system shown in Figure 3.3(a) to EV regenerative braking

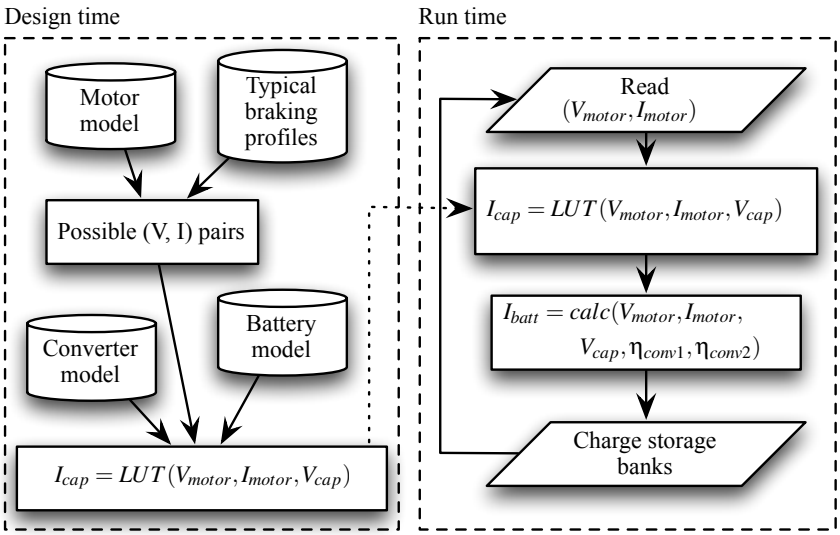

Figure 3.4 The proposed MPTT of regenerative braking [13].

system shown in Figure 3.3(b). The MPTT mandates to keep up with the optimal charging setup of the supercapacitor and battery banks during the entire braking process. We find that supercapacitor-battery HESS offers potentials for improving energy efficiency in such situations.

3.4.2 Regenerative Braking Framework

In this section, we introduce framework for regenerative braking MPTT with HESS. Figure 3.4 shows the design framework of the proposed MPTT for regenerative braking. The approach is look-up table (LUT) based. We assume that the overall system is roughly memory-less so that the framework is capable of making optimal decision based on the current EV status only. This statement is valid as the component models introduced in Section 5.3.2 are memory-less, that is, the efficiency values depend on current status only.

The framework consists of two parts, which are design-time procedure and run-time procedure. The objective of design time procedure is to build a LUT to be used on run-time. The inputs for the procedure are the i) motor/converter-/battery model and ii) typical braking patterns of a vehicle. First, using the motor model from Section 5.3.2 and the braking pattern, which consists of typical torque and RPM profile, the procedure obtains several pairs of motor output voltage and current within a feasible range during regenerative braking process. This (V_{motor}, I_{motor}) pair, the rectified motor voltage and current, becomes an entry for the LUT. Supercapacitor SOC, represented by its terminal voltage V_{cap}, becomes the third entry for the LUT. The content of the LUT is the optimal supercapacitor charge current for given V_{motor}, I_{motor}, V_{cap} tuple. The optimal value of the supercapacitor charge current is found by exhaustive search at design time. The solution search time is adjusted by the quantized levels of the input entries.

$$I_{batt,bus} = \eta_{conv}(V_{motor}, V_{batt}, I_{batt}), \tag{3.1}$$

$$I_{cap,bus} = \eta_{conv}(V_{motor}, V_{cap}, I_{cap}), \tag{3.2}$$

$$I_{motor} = I_{cap,bus} + I_{batt,bus}, \tag{3.3}$$

where $I_{cap,bus}$, $I_{batt,bus}$ are the converter input current values for each ESS bank. We exclude batteries voltage from the LUT entry without loss of generality, because battery terminal voltage is almost fixed during the short time frame of single regenerative braking process.

We determine the optimal I_{cap} by the use of the lookup table. Besides, we calculate I_{batt} fast enough at run time because we have analytical model of the

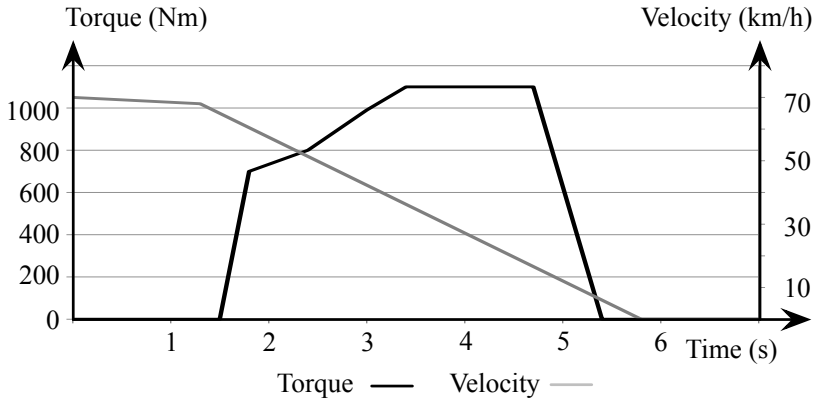

Figure 3.5 Braking profile of an EV from 70 km/h to 0 km/h [42].

converter efficiency.

3.5 Experiments

We show that the proposed MPTT method outperforms the conventional techniques that maintain a constant battery current [36] or the supercapacitor first policy [12] in various types of vehicles. In this section, we look into three distinguishing types of EVs, Toyota Prius Plug-in Hybrid, Nissan Leaf and Tesla Model S. All of the vehicles equip Li-ion battery of size 4.4 kWh, 24 kWh, and 60 kWh. Other vehicle parameters are covered in Section 2.

We use regenerative brake profile from [42] shown in Figure 3.5, which is a rapid braking scenario of an EV slowing down from 70 km/h to 0 km/h within 8 seconds. The torque and velocity values are for the wheel side, which means that the actual torque and RPM of the motor differs according to the axle ratio of each vehicle. Recall Figure 3.1 and only the regenerative braking portion of the total braking force is shown in the resultant figures.

We have implemented the experimental framework in MATLAB environment. The battery bank parameters are set to resemble each type of vehicle as discussed above. For the supercapacitor bank, we assume a supercapacitor bank of 300 cells connected in series to form 3 F, 750 V maximum voltage. The capacitance values is smaller than the one used in previous research, which is 7 F from [17], however, the higher terminal voltage ensures sufficient capacity for one time acceleration and deceleration of the EVs in interest.

The details of the baseline algorithms are as follows.

Battery constrained policy: Battery-constrained policy puts priority on the battery charge power. However, the battery bank efficiency degrades significantly in high current scenarios, so that we impose a upper limit on the battery current. We set it to be 2C that the charge power capacity of the battery is sufficient enough to retrieve the regenerative braking power while limiting the power loss from high currents. The regenerative power, which cannot be handled by the battery goes into the supercapacitor bank. We assume that the supercapacitor has enough residue capacity so that it does not reach its maximum voltage.

Supercapacitor first policy: Supercapacitor has very high power capacity, which make it suitable for handling high peak currents during rapid braking. This policy puts priority on the supercapacitor charge current. However, excessive current into the supercapacitor, especially when the terminal voltage is low, can be harmful to the overall energy efficiency.

The resulting profiles for Toyota Prius Plug-in Hybrid, Nissan Leaf and Tesla Model s are shown in Figures 3.6, 3.7 and 3.8, respectively. The trend significantly differs according to the type of vehicle. First, Prius has a relatively

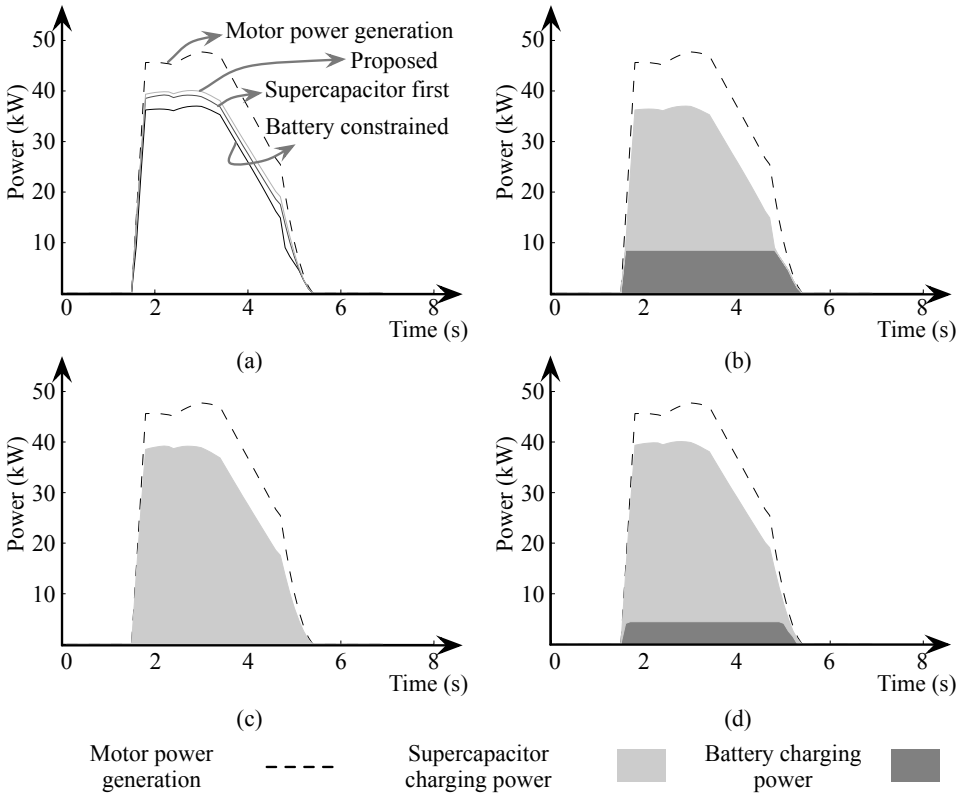

Figure 3.6 Charging power profile for Toyota Prius Plug-in Hybrid-sized HESS. (a) Total charging power. Charging power profile for (b) battery constrined, (c) supercapacitor first, and (d) proposed policy.

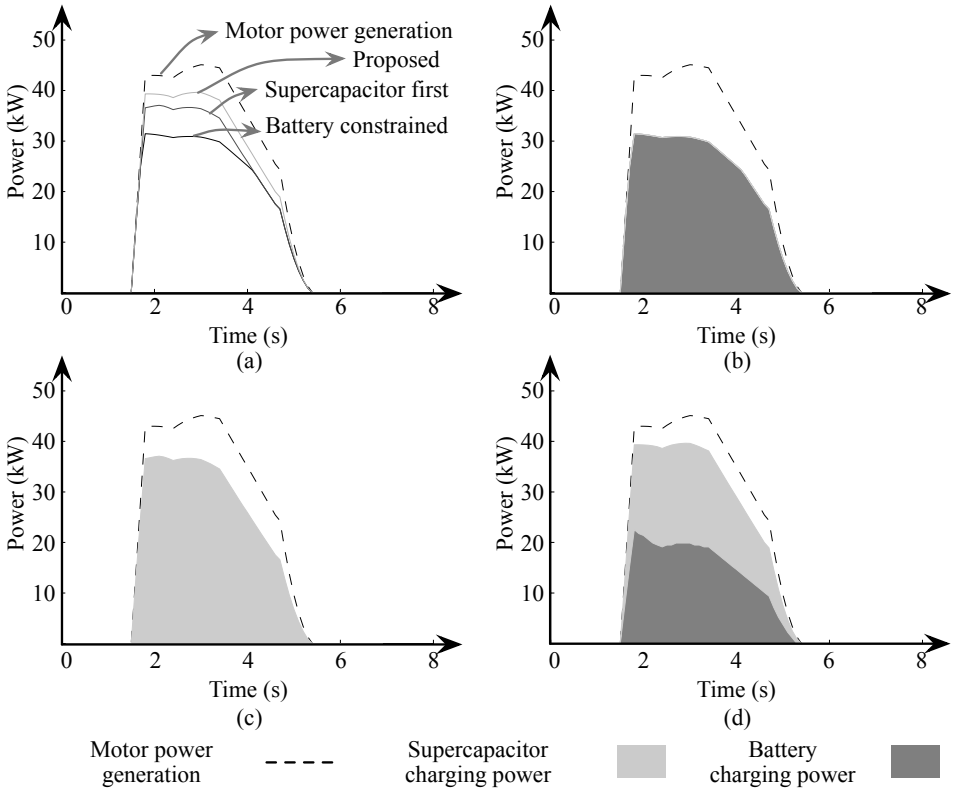

Figure 3.7 Charging power profile for Leaf-sized HESS. (a) Total charging power. Charging power profile for (b) battery constrined, (c) supercapacitor first, and (d) proposed policy.

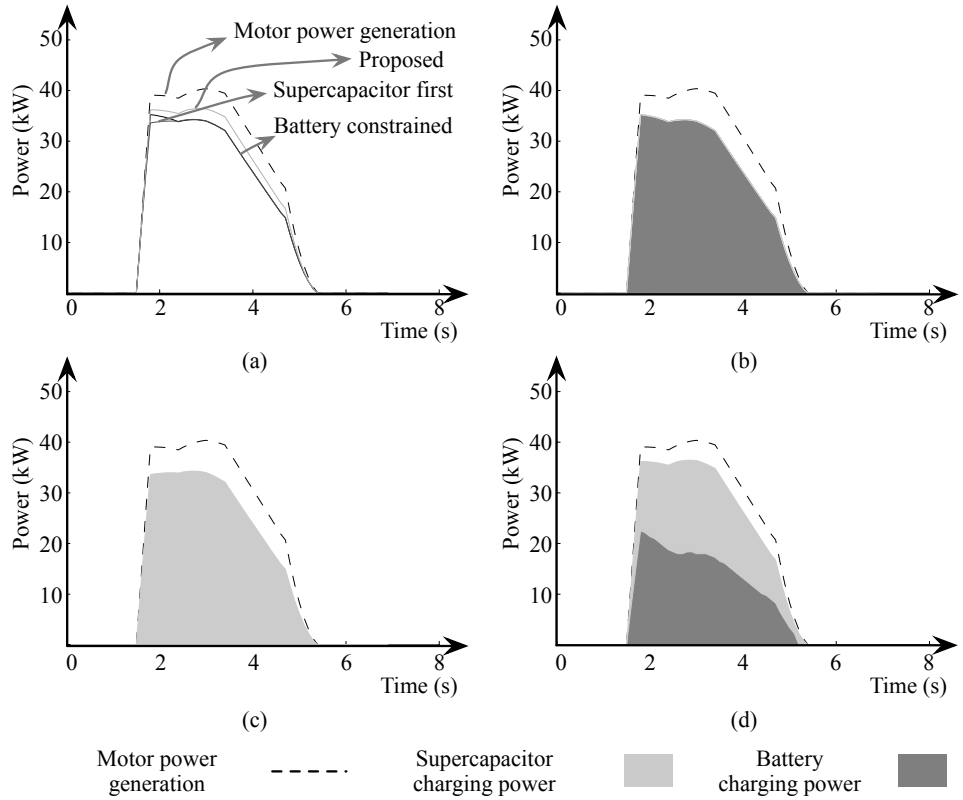

Figure 3.8 Charging power profile for Tesla Model S-sized HESS. (a) Total charging power. Charging power profile for (b) battery constrined, (c) supercapacitor first, and (d) proposed policy.

small capacity battery of size 4.4 kWh. The power capacity of the battery is not high enough to store the regenerative braking power efficiently. Thus, inefficiencies due to 2C charging current of the battery becomes a limiting factor for the first baseline. The second baseline performs slightly better than the first baseline in that the it removes inefficiency resulting from the rate capacity loss. The proposed technique exhibits better efficiency because it removes the burden of the supercapacitor bank charger, which is handling 150 A current in the second baseline. The propose technique determines the battery charge current to be around 1C where its efficiency is very high and lets the supercapacitor to handle rest of the power. Second, Nissan Leaf has a quite large battery of size 24 kWh. The battery current limit of 2C is large enough to handle the regenerative braking power with reasonable efficiency. The first and second baseline shows comparable efficiency, yet the supercapacitor first policy shows slightly higher efficiency due to supercapacitor's superior cycle efficiency. The benefits of the proposed algorithm comes from both the superior cycle efficiency of the supercapacitor and increased efficiency of the supercapacitor charger. Third, Tesla Model S has the largest battery of size 60 kWh. The cycle efficiency of the battery is almost 100% so that the performance of the first and second baseline is almost the same. The benefit of the proposed algorithm mainly comes from improved DC–DC converter and charger efficiency of the ESS banks. Balancing the use of the battery and supercapacitor makes the chargers of the two ESS banks to operate in a higher efficiency region.

Chapter 4

Proactive Charge Management in Electric Vehicle HESS

4.1 Potentials of Proactive Charge Management

This chapter focuses on SOC management of HESS in EVs from a perspective of driving cycles. The previous chapter has shown that the regenerative power generation pattern, conversion efficiency, and energy storage element plays an important role in energy efficiency. However, the previous problem is rather focused on optimizing short-term instantaneous energy efficiency, and this type of management does not lead to globally optimal charge management. For example, suppose an EV equipped with supercapacitor-battery hybrid is accelerating from gradually for the first 10 seconds and rapidly the following 5 seconds. If a charge management algorithm utilizes supercapacitor in a greedy manner such that its SOC becomes nearly empty at 10 seconds, energy efficiency during rapid acceleration in the last 5 seconds could be degraded. Thus, a charge manage-

ment technique considering the energy efficiency for a certain period of time is important for achieving globally optimal solution. In this chapter, we propose a proactive charge management technique, which improves energy efficiency in a driving cycle comprising of braking, stopping/cruising, and acceleration stages. Proactive charge migration requires some sort of forecast of driving pattern, where our techniques achieves this by the use of GPS navigator. The proposed method more efficiently enhances effective gas mileage of EV with accurate prediction of the vehicle route and traffic conditions. Manual driving nowadays is largely relied on a GPS navigator, a semi-autonomous driving such as adaptive cruise control utilizes the traffic condition via onboard radars, and autonomous driving even more utilizes computerized traffic information. Therefore, it is not surprising to have traffic and driving information and predict the near future driving patterns available.

4.2 Hybrid Energy Storage Systems for Electric Vehicle

4.2.1 EV HESS Topology

Despite the high degree of freedom HESS architecture offers, the topology of HESS for EVs is subject to tight constraints in weight and volume. Typically, ESS for EV is a homogeneous Li-ion battery bank, which is by far the best type of energy storage element overall especially in terms of energy density, and cycle efficiency. Adding another type of bank mandates addition peripheral circuitry such as BMS, which could be a significant burden for an EV. Therefore, it is not recommended to install an excessively large supercapacitor in an EV. We assume that the capacity of the supercapacitor is designed to accommodate

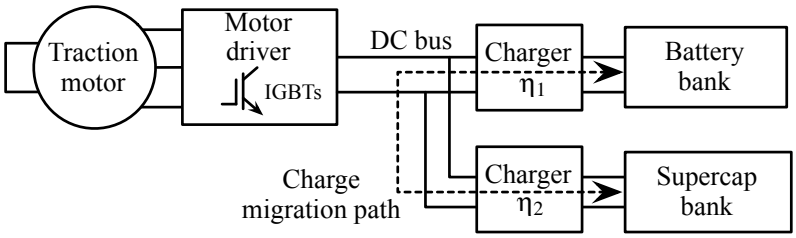

Figure 4.1 EV HESS topology and charge migration.

average energy capacity for only one time acceleration or deceleration. Thus, most HESS for EVs assume simplest battery-supercapacitor topology shown in Figure 4.1. The battery bank and supercapacitor bank is connected via DC bus to the motor driver and traction motor. Some previous works consider direct parallel connection of battery and supercapacitor without chargers. However, the topology poses a lot of stress on the battery bank, and offers no freedom of control for systematic optimization, so exclude it from discussion.

4.2.2 EV HESS Charge Management

Charge replacement, allocation and migration occurs during EV acceleration, deceleration, cruising and stopping. Charge replacement takes place during acceleration phase. The motor becomes the electrical load. Charge allocation occurs during deceleration phase. The motor becomes the power source in this case supply regenerative braking energy to the energy storage banks. Charge migration can take place anytime during driving. Charge migration path in EV HESS is shown in Figure 4.1.

A greedy charge management policy may choose the destination EES banks only based on their instantaneous charging/discharging efficiency. For example, such a policy tries to charge EES banks with a high power capacity such as a su-

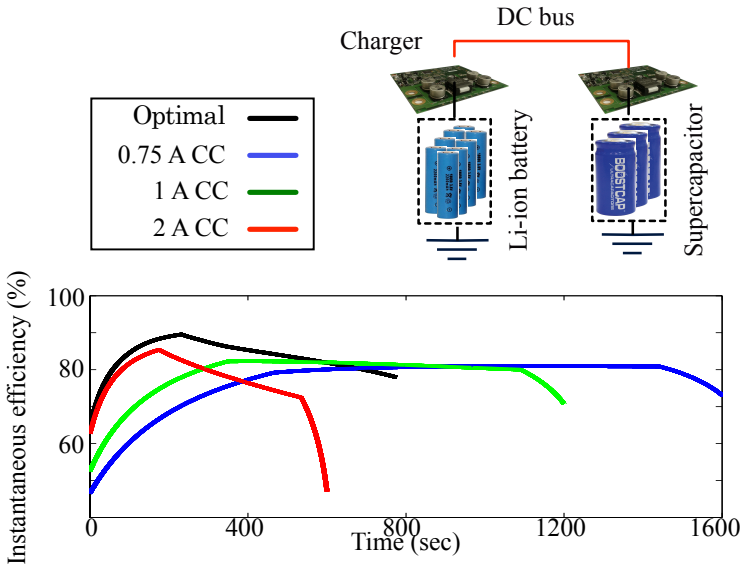

Figure 4.2 Battery bank to supercapacitor bank migration efficiency example.

percapacitor bank. Supercapacitor banks generally have a low energy capacity and soon will be fully charged at the beginning of the charge allocation process. The rest of charge allocation process should charge other battery banks, which results in a low overall efficiency. The voltage on the CTI significantly change the efficiency of the chargers, which should be carefully determined by the input source voltage and the destination bank voltage. The optimal charging/discharging current and the CTI voltage changes over time as charge allocation progresses. We continue to monitor, calculate the optimal setup and control the charge allocation process accordingly [69, 63, 68, 64]. Elaborated charge management policies shown in Figure 4.2 improves efficiency up to 30% comparing with conventional homogeneous ESS systems [69].

In this chapter, we rely on our previous works for the detailed algorithms for charge replacement, allocation, and migration. A near optimal charge re-

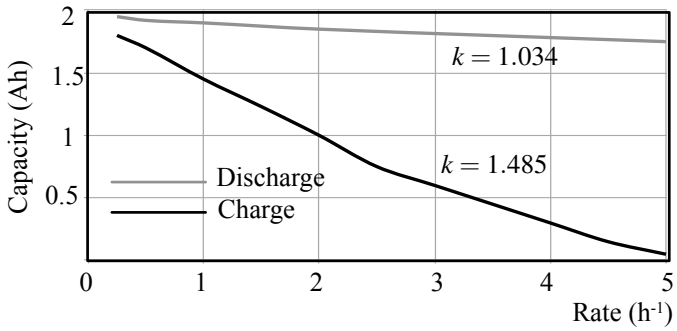

Figure 4.3 Peukert plot of a 1.9 Ah 18650 Li-ion cell [18].

placement algorithm can be used during the acceleration phase [69]. Charge allocation algorithm during vehicle deceleration is adopted from the algorithm used in Chapter 3. We also consider charge migration for further efficiency improvement based on algorithm from [63]. Charge migration can be beneficial under certain circumstances of EV. For example, in cold start up situation, supercapacitor would be empty and sudden acceleration results in drawing large current from the battery bank. After driving is over, electrical energy remains in the supercapacitor, which is susceptible to high self-discharge rate of supercapacitors. For both cases, it is better to migrate charge from one to another for energy efficiency. However, cold start and after-drive conditions are not the only scenarios that migration can take effect as we will discuss in the following section.

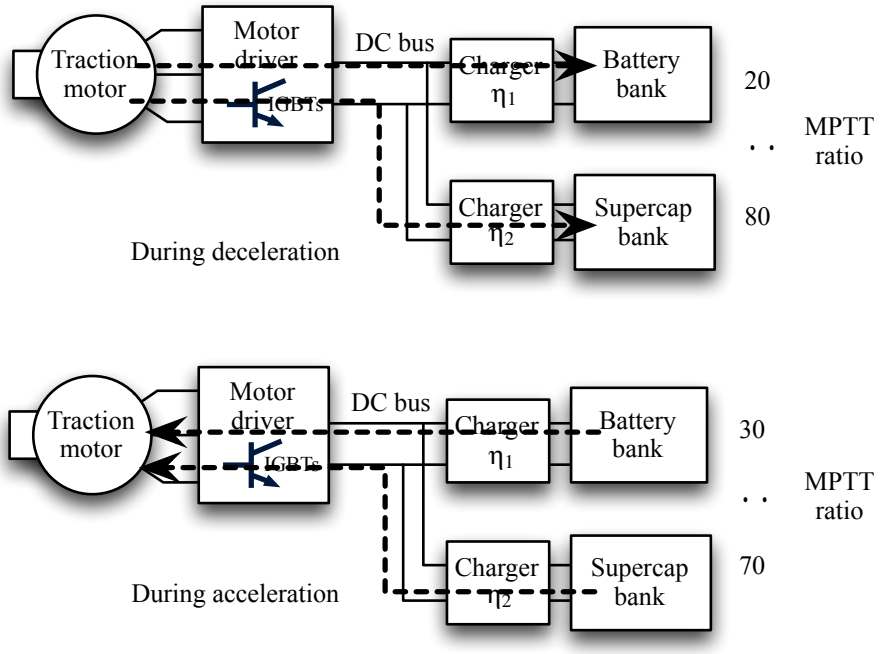

Figure 4.4 Charge imbalance example due to battery asymmetry during charging and discharging.

4.3 Battery Charging and Discharging Asymmetry and Charge Migration

We made an observation from Section 2.2.3 that there is significant asymmetry in battery charging and discharging. Rate capacity effect during battery charging is even more severe as shown in Figure 4.3. Charging current of 2C gives more than 30% degradation in usable capacity. This becomes a significant problem during regenerative braking efficiency, where the battery charging current goes up to a few C during rapid deceleration.

The optimal discharge current of both banks during acceleration differs from the optimal charging current during regenerative braking, which implies

imbalance in ratio of net power between the battery bank and supercapacitor bank as shown in Figure 4.4. Charge migration mitigates inherent asymmetry in ESS charging/discharging behaviors during acceleration and deceleration of the EV. We make use of the idle and cruise periods of the EV to perform proactive charge migration. In other words, we decouple the acceleration and deceleration optimization, which was coupled by the SOC management of the supercapacitor in the previous works. By applying charge migration from the supercapacitor to battery while stopping or cruising, and the charge migration manages the supercapacitor SOC without sacrificing the energy loss during acceleration and regenerative braking.

4.4 Charge Management Efficiency Enhancement Problem

We formulate EV energy efficiency enhancement problem as optimization for given driven profile. Enhancement of the energy efficiency is equivalent to increasing the SoC remaining in the HESS at the end of given driving profile is executed. We make a discrete time approach and divide the driving profile into N equal time slots. The define E_{HESS} as the optimization objective defined as

$$E_{HESS}[N] = E_{bat}[N] + E_{cap}[N], \tag{4.1}$$

where $E_{bat}[N]$, $E_{cap}[N]$, N are energy remaining in battery bank at Time Slot N, energy remaining in the supercapacitor at Time Slot N.

We define efficiency of the two chargers and motor driver as a function of battery voltage (V_{bat}), battery current (I_{bat}), supercapacitor voltage (V_{cap}),

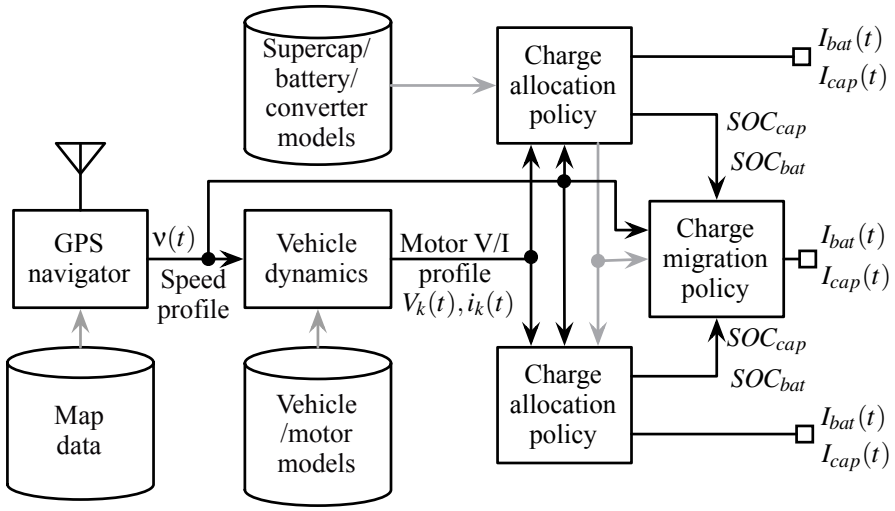

Figure 4.5 EV HESS management framework.

supercapacitor current (I_{cap}), DC bus voltage (V_{bus}), motor RMS voltage per phase (V_k), and motor RMS current per phase (i_k). We assume that the hydraulic braking force profile during braking is given so that the torque and angular velocity of the motor and thus the voltage and current of the motor can be obtained from the vehicle speed profile using vehicle dynamics and the torque-current model of the motor in Section 2.1.

4.5 EV HESS Management Policy

We deliberately take advantage of charge migration in EV HESS charge management. Figure 4.5 demonstrates the framework of the proposed EV HESS management. The pseudo code for overall charge management algorithm is described in Algorithm 1. The inputs for the algorithm are driving profile forecast for one deceleration and acceleration cycle and initial SOC of the battery and supercapacitor banks. We denote T_0, T_1, T_2, and T_3 as forecasted braking start

Algorithm 1: EV HESS SOC management algorithm for one deceleration-acceleration cycle.

Input: Driving profile forecast ($\tau_{motor}(t)$, $\omega_{motor}(t)$) for one cycle, initial battery and supercapacitor SOC values $SOC_{bat}(T_0)$, $SOC_{cap}(T_0)$

Output: SOC_{bat},SOC_{cap} for every time slot.

1 ($V_m(t)$, $I_m(t)$)← motorModel($\tau_{motor}(t)$, $\omega_{motor}(t)$)

2 Find braking end time T_1

3 ($SOC_{bat}(t)$, $SOC_{cap}(t)$)←Allocation(V_m, I_m, $SOC_{bat}(T_0)$, $SOC_{cap}(T_0)$, $T_1 - T_0$)

4 Find acceleration start time T_2 end time T_3

5 ($SOC_{bat}(T_2)$,$SOC_{cap}(T_2)$)← $\underset{SOC_{cap}(T_3)=SOC_{cap,min}}{FindArg}$ Replacement(V_m, I_m, $SOC_{bat}(T_2)$,$SOC_{cap}(T_2)$,$T_3 - T_2$)

6 ($SOC_{bat}(t)$, $SOC_{cap}(t)$)← chargeMigration($SOC_{bat}(T_1)$,$SOC_{cap}(T_1)$,$SOC_{bat}(T_2)$,$SOC_{cap}(T_2)$,$T_2 - T_1$)

time, braking end time, acceleration start time, and acceleration end time, respectively. As we perform migration in between, charge allocation and replacement are decoupled and optimized in a separate manner. The algorithm runs Allocation() function, which denotes charge allocation algorithm from Chapter 3, from T_0 to T_1. The result of line 3 is SOC profiles of both banks. Then the algorithm runs Replacement() function, which denotes charge replacement algorithm from [69]. This time, however, the purpose is to find arguments for Replacement() function that satisfies $SOC_{cap}(T_3) = SOC_{cap,min}$. The result of line 5 is ($SOC_{bat}(T_2)$,$SOC_{cap}(T_2)$). As we assume that the capacity of the supercapacitor is designed to accommodate average energy capacity for only one time acceleration or deceleration, condition $SOC_{cap}(T_3) = SOC_{cap,min}$ is valid[1]. By line 6, we have the initial and final conditions of the charge migration problem, which occurs during T_1, T_2 as the final status of the charge allocation problem, and the terminal conditions as the initial status of the charge replacement problem, and apply charge migration algorithm in [63]. The functions Allocation(),

[1]We cannot fully empty the supercapacitor because the power converter requires a certain minimum input voltage.

Replacement(), and Migration() considers most non-ideal characteristics of the power converter and battery considering the DC bus voltage, supercapacitor bank current, and battery bank current to derive the optimal supercapacitor and battery charge currents. The charge migration algorithm tries to evenly distribute the migration current as much as possible over time while considering the efficiency of the converters. The optimal charge allocation and replacement of EV are not symmetrical even though we apply a symmetric deceleration and acceleration profiles. The final supercapacitor and battery SOC at the end of charge allocation is generally different from the initial supercapacitor and battery SOC at the beginning of charge replacement. The major reasons that cause such asymmetry include battery asymmetry discussed in Section 2.2.3, existence of hydraulic brake force, and so on. However, the proposed method is able to provide superior energy efficiency because charge migration fills the gap between charge replacement during acceleration and charge allocation during deceleration supercapacitor SoC requirement. The underlying assumption here is that we know the vehicle behavior in the near future using GPS navigator and semi-autonomous driving features discussed in Section 4.5.

4.6 Experiments

We validate the proposed approach by simulation through a commercial EV on standard driving cycles. The target vehicle is a 5-door hatchback full-EV Nissan Leaf. Nissan Leaf is equipped with an 80 kW, 280 N·m electric motor, a 24 kWh Li-ion battery, weighs 1521 kg, has an axle ratio of 7.94:1, and drag coefficient of 0.28. Other parameters required to calculate the electrical outputs of the motor from the driving profile are extracted from other cars of similar

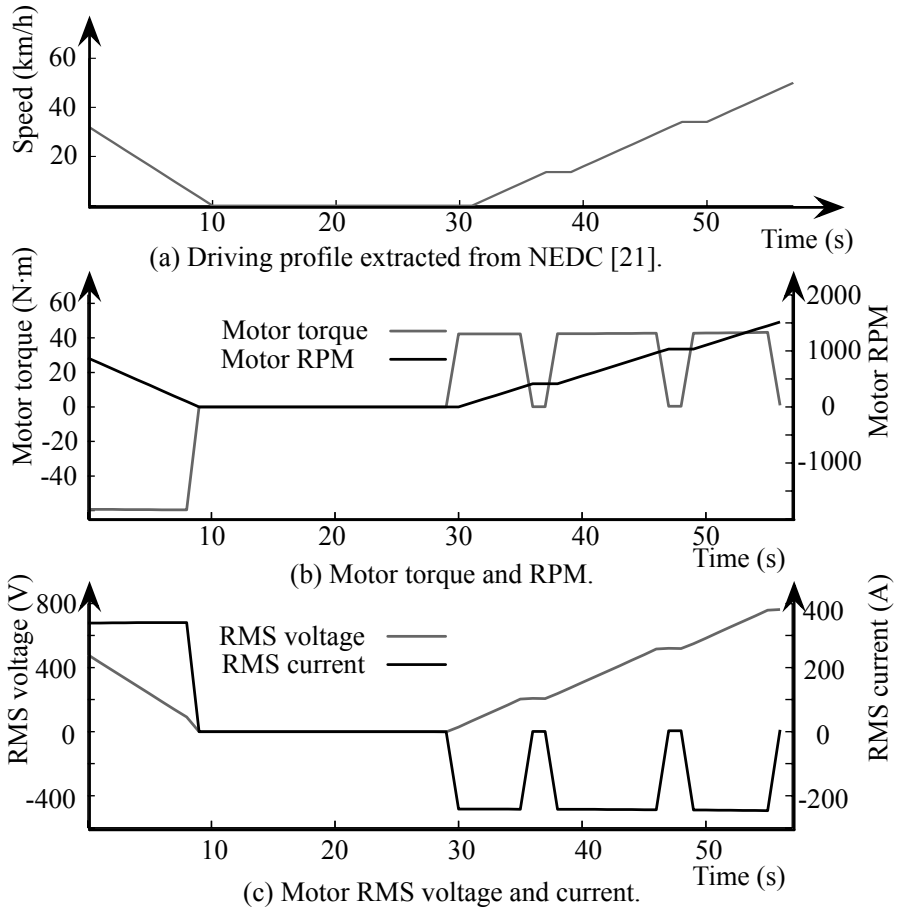

Figure 4.6 Driving cycle and motor trace.

size. The size of the supercapacitor is 15 F, which is similar to the capacity used in previous works on battery-supercapacitor HESS for EV [40]. It consists of 200 series connection of 3000 F supercapacitors to exhibit maximum voltage of 500 V. The driving profile we used for simulation is shown in Figure 4.6(a). It is a part of the driving cycle, ECE-15 UDC (Urban Driving Cycles), in standard driving profile NEDC (New European Driving Cycle) [1]. Figures 4.6(b) and 4.6(c) show the motor torque, motor RPM, RMS voltage, and the RMS current

of the electric motor calculated from the equations in Section 2.1. The baseline policy for comparison is balanced charging/discharging during deceleration and acceleration without active migration. Figure 4.7 shows the experimental results for the proposed and baseline policies. The ESS receives the regenerative braking energy from 0 s to 10 s. The charging profile of the ESS controlled by MPTT technique during the period is the same both for the proposed and baseline. However, the proposed policy performs gradual migration from the battery to supercapacitor during 10 s to 30 s to prepare for acceleration in 30 s to 50 s as opposed to the baseline policy. The acceleration of the EV is much supported by supercapacitor discharge power, which beneficial for the overall energy efficiency. The proposed policy consumes 19.4% less energy (1643 kJ) than the baseline (2013 kJ) for the same profile.

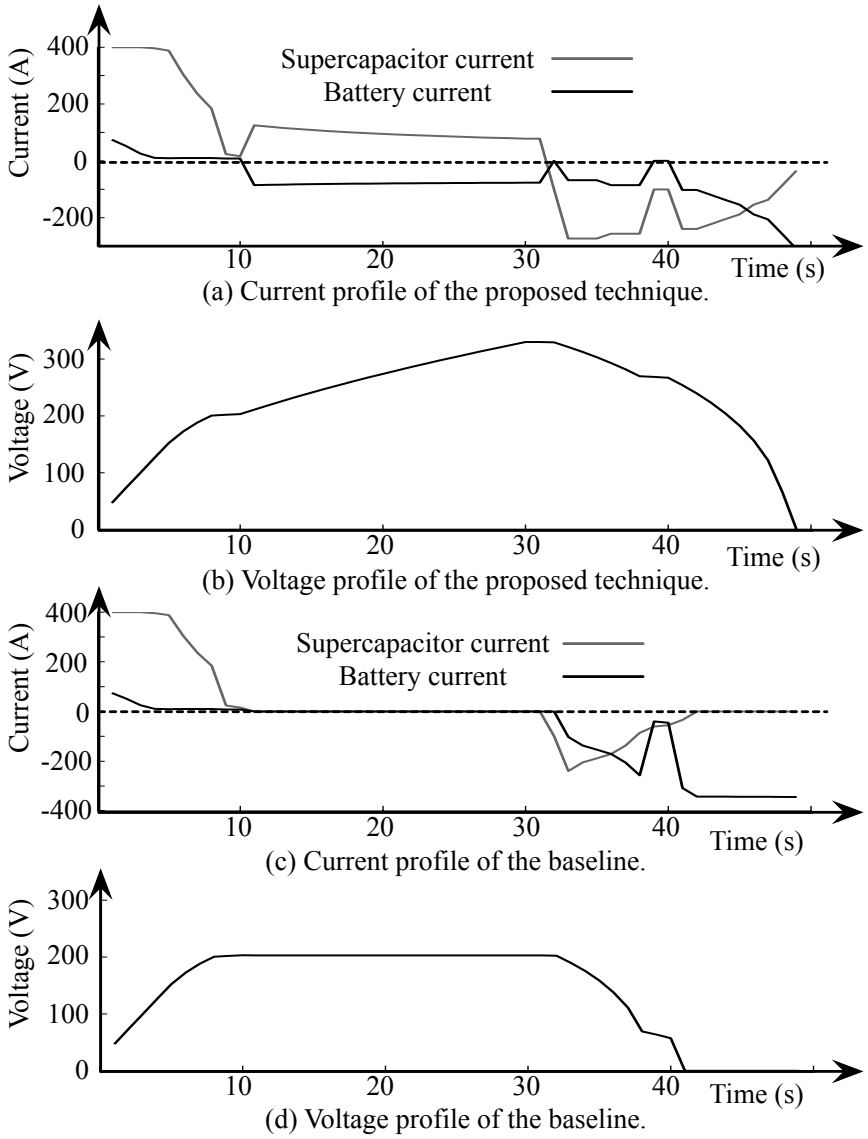

(a) Current profile of the proposed technique.

(b) Voltage profile of the proposed technique.

(c) Current profile of the baseline.

(d) Voltage profile of the baseline.

Figure 4.7 Experimental results ($C = 15$ F).

Chapter 5

Electric Vehicle Charging Cost Reduction

This chapter studies impacts of EV charging on grid and proposes a EV charging algorithm capable of minimizing the electricity bill. Prior works discussed in Section 2.4 showed that impact of EV charging on the grid will be critical as the number of EVs are expected to increase rapidly. The benefits of EVs diminish without proper considerations in the grid side. First, the claimed low carbon emission is no longer valid if the grid relies on dirty electricity sources such as coal. So it is advisable to use as much renewable energy or any other forms of clean power source as possible. Second, claimed low cost per mile is no longer valid if the utility companies begin to apply normal rates to electricity charging. Pricing policy of the electricity is closely related to the types of load. For example, residential electricity price provided by Los Angeles Department of Water and Power (LADWP) is only 23.775 cents per kWh even at the very peak period during summer. The average residential load demand per household

is at most a few kilowatts. However, when the EV charging comes into the picture, the load shape becomes completely different. EV ESS has a very large capacity and its charging requires significant amount of power. Depending on the charging standards, the charging power could easily exceed tens of kilowatts, which would impose significant burden for the residential EV charging stations in the near future. In the chapter, we devise a EV charging algorithm capable of minimizing the electricity bill where the unit cost of electricity changes over time. The target residential electric system is powered by PV cells as well as the grid. Usage of PV cells helps achieve both low carbon emission and operating cost of EVs.

5.1 Electric Vehicle Charging Standards

Full EVs and plug-in hybrid vehicles are charged from the grid. There are various standards of EV charging as shown in Figure 5.1.

AC Level 1: AC level 1 charging provides charging through 120 V AC plug and requires electrical installation per National Electrical Code. All EVs come with an AC level 1 electric vehicle supply equipment (EVSE) cordset that no additional charging equipment is required. The typical charging power for level 1 charging is 2.4 kW, which takes about 10 hours for a Nissan Leaf-sized FEV to charge until full.

AC Level 2: AC level 2 charging provides charging at 240 V (typical in residential applications) or 208 V (typical in commercial applications). AC level 2 EVSE requires installation of a dedicated charging equipment typically capable of supplying 7 kW power to the EV ESS. This means that Nissan Leaf-sized FEV takes 3 hours until full charge.

(a)

(b)

(c)

Figure 5.1 Various charging standards. (a) AC level 1 charging. (b) AC level 2 charging. (c) DC fast charging.

DC fast charging: DC fast charging provides highest charging power of up to 50 kW at 480 V. This also requires a dedicated charging equipment. Unlike other charging standards DC fast charging is capable of charging the EV ESS up to 80% because the last 20% takes a long time. DC charging is capable of charing Nissan Leaf-sized FEV to 80% charge in 20 minutes.

We consider EV being charged during night time at AC level 1 and AC level 2 charging standards in this chapter.

5.2 Residential Photovoltaic Installations and EV charging

The number and capacity of photovoltaic (PV) power system installations are increasing rapidly. Cumulative installations of these systems, which are mainly Grid-connected, have reached 2.15 GW_{DC} in the US alone. Residential PV installations increased at a year-over-year rate of 64% and accounted for 29% of all PV installations in 2010 [4]. However, the growth rate is still slower than desired despite the many advantages of PV systems. This is because of the long break-even time for such systems (the time that is needed for customers to save enough money with lower monthly electricity bills to compensate the initial cost of purchasing and installing the PV system). Maximizing the benefit from the PV system, which is lower electricity bill, is equally important to reducing the installation cost to shorten the break-even time.

Moreover, minimizing the electricity bill reduces operating cost of EV. Plug-in EVs require charging from the grid, which will eventually become a significant burden for the EV owners. Making use of residential PV installations as an energy source for the EV charging is beneficial in terms of carbon emission, energy efficiency and electricity bill reduction. Using residential PV power reduces the power generation and transmission efficiency discussed in Section 1.1. Electricity bill reduction comes from the PV power, which is free once installed.

Many previous studies on solar powered systems focused on enhancing the efficiency of the PV system components such as the PV array and PV inverters. The mainstream research is related to maximum power point tracking (MPPT) methods that ensure maximum PV output power in spite of variable solar irradiance [22]. Recent work has presented a maximum power transfer tracking

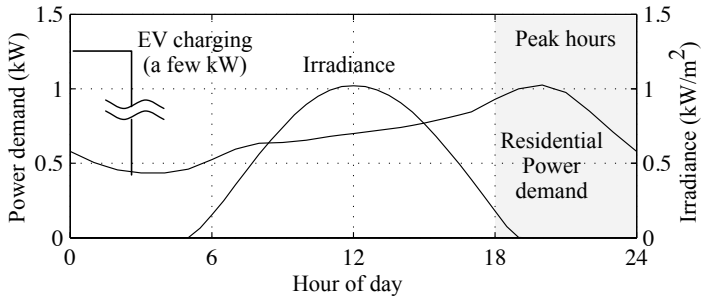

Figure 5.2 PV array output power, hourly average residential load profile (Southern California Edison territory) [2] and EV charging power.

(MPTT) method to maximize the actual energy delivered from a PV array into an energy storage device, considering the power conversion losses [30].

Grid-connected PV systems without a battery do not require elaborate management. Simply performing MPPT or MPTT, and consuming the PV power first and the Grid power second has been sufficient for cases where the PV power is smaller than the load power. Similarly, standalone PV systems equipped with a battery [7, 53] can use a simple policy in which the battery is charged during the day and discharged during the night. In contrast, Grid-connected PV systems should consider complex scenarios such as using the electrical energy stored in the battery when the electricity price is high, i.e., during peak power consumption hours. However, one of the major hurdles in reducing the electricity bill is the mismatch among the PV power generation, load demand, and electricity prices. Figure 5.2 shows that the peak solar irradiance occurs at noon while the peak residential load demand is at 8pm. EV charging takes place during the night where an EV is not used and docked into a charging facility at home. Many electricity providers sell the electricity at higher price during the peak hours to control the peak power demand. For example, unit electricity

price in the greater Los Angeles are during the peak hours is as much as three times that during the off-peak hours [34]. Grid-connected PV systems without a battery can hardly cope with the peak-hour load demand.

Grid-connected PV systems with a local battery are one way to significantly enhance the usefulness of the solar powered system because it can cope with the peak-hour load demand. Knowing when to charge and when to discharge the battery is the key to success of Grid-connected PV systems with a battery. However, most previous work performs battery management without employing systematic optimization and/or optimality consideration in spite of the significant amount of relevant work. For example, early work simply limits the battery current and considers reselling the excess energy from the PV system to the Grid [41]. *Power leveling*, which controls the power drawn from the Grid [14], and *peak shaving* [25] can mitigate the problem, but they do not provide systematic optimization of the system efficiency or the billing cost. There is a systematic optimization based on Lagrangian relaxation method, but it focuses on issues from the power distribution network such as locational marginal pricing (LMP) and transmission congestion problems [35]. Recent work provides an algorithm that determines when and how to charge and discharge the battery, but the method is ad-hoc without much reasoning about the optimality [27]. An electricity bill minimization algorithm similar to our work has been proposed in [26]. However, the work assumes a different electricity billing policy based on the peak power usage, which makes the proposed algorithm essentially a peak shaving algorithm. Moreover, this work does not consider the rate of PV power generation. In contrast, our work focuses on minimizing the mismatch between the PV power generation and the load demand in a grid-connected PV powered

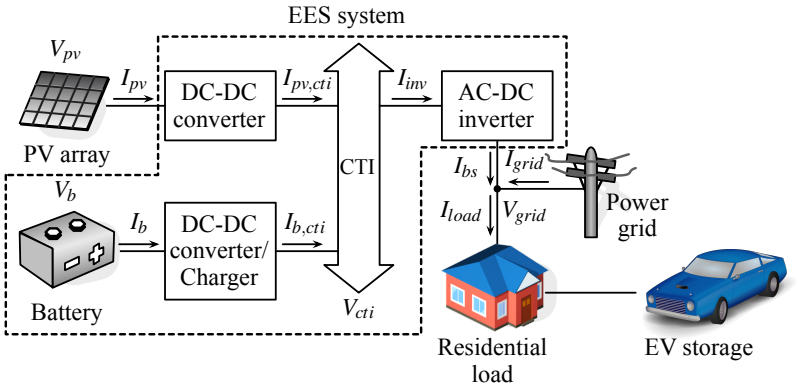

Figure 5.3 Residential PV system with support for EV charging.

home to minimize the electricity bill.

This chapter introduces a holistic optimization framework for battery-equipped residential Grid-connected PV power systems supplying power the both the residential load and EV charging demand. Unlike previous work, we develop a systematic optimization method for the battery management, which can effectively mitigate the electricity demand and supply mismatch. We devise an algorithm that determines when and how to store and retrieve energy from the battery to minimize the electricity billing cost. The proposed framework take into account the PV module impedance, converter loss, battery rate-capacity effect, and storage capacity limit for given solar irradiance, load profile, and billing policy. Experimental results show that our technique is capable of reducing up to 28% electricity bill when compared with previous battery management policies.

5.3 Grid-Connected PV System with a Battery

5.3.1 System Architecture

Figure 5.3 illustrates the overall system architecture considered in this chapter. We consider household-scale power consumption as the load. The load is powered by the PV array, power grid, or both. It has an energy storage means to eliminate/reduce the mismatch between power generation and power demand. The energy storage means comprises a battery module to be charged from the Grid when the electricity price is low and from the PV array when the load power is lower than the PV generated power. Together with the Grid, the battery module supplies power to the load device during the peak hours.

The battery module consists of a DC-bus that delivers power to and from the power source, a battery bank, and the load devices. Charging and discharging processes are controlled by a DC–DC converter, a DC–AC inverter, and a charger. This architecture allows use of multiple energy storage banks, even heterogeneous banks, in order to enhance the performance metrics such as power and energy capacity, cycle efficiency, and lifetime [43]. In this chapter, a single battery bank is installed.

5.3.2 Component Models

Photovoltaic array

Ideal power source can provide unlimited power capacity and constant voltage or current generation regardless of the environmental and load conditions. The PV array power capacity can be lower than its maximum value due to the environmental conditions such as solar irradiance and temperature. The output voltage of the PV array changes significantly as a function of the load

current. We use a single-diode equivalent circuit model [61] and consider such characteristics to maximize the energy efficiency of the system. We keep the PV system efficiency at the maximum, by performing the maximum power transfer tracking introduced in [30].

Converters and inverters

The target system consists of two switching power converters that connect the battery to a DC-bus: one for charging the bank and the other for discharging the bank. The PV array also connects to a DC–DC converter, which converts the DC voltage from the PV array to the DC-bus voltage. There also exists a DC–AC inverter and a rectifier for power delivery between the DC-bus and the Grid, respectively. *Efficiency* of a converter or inverter is defined as

$$\eta = \frac{P_{out}}{P_{in}} = \frac{P_{in} - P_{loss}}{P_{in}} = \frac{V_{in} \cdot I_{in} - P_{loss}}{V_{in} \cdot I_{in}}, \tag{5.1}$$

where P_{in} and P_{out} denote input and output power levels of the converter, respectively, and P_{loss} is the power loss in the converter/inverter. The power loss of a switching power converter comprises three components: conduction loss P_{cdct}, switching loss P_{sw} and controller loss P_{ctrl} [15] such that

$$P_{loss} = P_{cdct} + P_{sw} + P_{ctrl}. \tag{5.2}$$

The conversion efficiencies of the DC-AC inverter and rectifier can be modeled in a similar way as (5.2) except that there are additional components P_{trans}, and P_{filter}, which are the power losses from transformer and filters, respectively. The power loss for inverter is given as

$$P_{loss} = P_{cdct} + P_{sw} + P_{ctrl} + P_{trans} + P_{filter}. \tag{5.3}$$

Table 5.1 Parameter values for converter/charger and inverter models.

	Converter / charger	Inverter
a_1	2.40E-1	1.78E-1
a_2	-6.63E-5	-3.96E-5
a_3	-5.45E-3	-5.97E-5
a_4	7.13E-4	7.00E-6
a_5	1.16E-2	6.07E-3
a_6	6.89E-3	1.03E-3
a_7	-3.6967E-2	-5.85E-3

The power loss components are strongly dependent on the input voltage V_{in}, output voltage V_{out}, output current I_{out}, and the circuit component properties. We derive a closed form expression for η as a function of V_{in}, V_{out}, and I_{out}. The details of power loss equations for each term in (5.2) can be obtained from [15], and that of inverters are from [31, 3]. We do curve fitting for the converter efficiency as a quadratic function, which can still accurately represent the power converter efficiency in terms of the input voltage V_{in}, output voltage V_{out}, output current I_{out} as shown in (5.4). We denote the equations for calculating efficiencies of the PV converter, battery converter, and inverter as η_{pv}^{out}, η_{b}^{out}, η_{inv}^{out}, respectively. Also, we can calculate the efficiency using the term of I_{in} instead of I_{out}. We denote the equations as η_{pv}^{in}, η_{b}^{in}, η_{inv}^{in}. The regression coefficient values for the quadratic equation are reported in Table 5.1.

$$\eta^{out} = a_1 V_{in}^2 + a_2 V_{out}^2 + a_3 I_{out}^2 + a_4 V_{in} + a_5 V_{out} + a_6 I_{out} + a_7. \tag{5.4}$$

Battery

Modeling the behavior of battery itself is a challenging task, which has been studied during the past few decades. Battery models from [50, 47] are mainly

based on electrochemical process modeling and analysis. Despite the accuracy of the models, they are too complex for use during the system-level design of electronics. Instead we rely on a circuit based model, which captures the most important battery behavior, i.e., the rate capacity effect. The rate capacity effect of batteries is described by the Peukert's formula,

$$\eta_{rate}(I) = \frac{k}{I^{\alpha}}, \tag{5.5}$$

where k and α are constants.

5.4 Electricity Bill Reduction

5.4.1 Power Generation and Usage Models

Residential electrical load demand is fairly periodic although it fluctuates greatly according to time of day. The periodicity of the usage patterns is closely related to consumers' livening patterns, including space heating, cooling, hot water usage, cooking times, television watching hours, EV charging patterns and so on. The hourly averaged residential load profile measured in Southern California shows that the peak value occurs at 8pm when residents come home from work [2]. The peak is 2.5 times higher than the minimum value. Many electricity providers sell electricity at different rates at different times of day to control the usage of electricity during peak hours. For example, unit electricity price in Los Angeles is 16.061 ¢/kWh during peak hours, and 4.655 ¢/kWh during off-peak hours [34]. Another important component of residential load in our setup is EV charging. According to the kind of charging standards discussed in Section 2.4, the peak load range from a few kW to tens of kW. An EV owner can charge the vehicle any time during the day, but we assume a situation where EV is parked

to the charging facility at home during the night, and charges around midnight where the grid electricity is the cheapest.

5.4.2 Battery Management for Electricity Bill Reduction

We minimize the electricity bill, which is the summation of Grid power usage multiplied by the unit cost. We consider two sources of power generation to demonstrate the proposed idea: a PV array and Grid. The optimal policy for the Grid-connected PV system without battery storage is to do maximum energy harvesting. For such systems, simply performing MPPT or MPTT will suffice [30]. On the other hand, achieving the goal of electricity bill reduction in a Grid-connected PV-powered homes with battery storage involves optimization from many aspects. Depending on the ratio between the peak hour and off-peak hour electricity prices, the in-home PV system may either supply power to the load or charge the battery during off-peak hours. Also, we charge the battery when the electricity is cheap and the PV power is not enough to fully charge the battery, preparing to use the battery to perform load shaving during the peak hours. However, charging the battery is less efficient than supplying power to the load due to the battery's internal resistance and charger power losses. Furthermore, high-current charging and discharging result in severe charging and discharging efficiency degradation due to the rate-capacity loss in the battery. We prohibit the case where the battery becomes fully charged and the PV power generation is higher than the load power consumption because we do not consider selling the PV power to the utility company not to lose generality. Not all the electricity companies buy PV power from individual residences.

5.4.3 Problem Formulation

The electricity bill minimization problem for Grid-connected residential PV power systems is formulated as follows.

Objective:

Minimize electricity bill for a day, that is,

$$cost_{day} = \sum_{n=1}^{N} C[n]p_{Grid}[n], \tag{5.6}$$

where $C[n]$ is the unit price of the Grid electricity (\$/kWh), $p_{Grid}[n]$ is the power drawn from the Grid (W) at time slot n, and N is the number of time slots per day.

Given:

- Solar irradiance profile for a day $G[n]$.
- Residential load demand profile for a day $I_{load}[n]$.
- Unit price of the Grid electricity $C[n]$.

Control variables:

- DC-bus voltage $v_{bus}[n]$.
- PV operating point $V_{pv}[n]$, $I_{pv}[n]$.
- Battery current $I_b[n]$, where $I_b > 0$ if discharging, and $I_b < 0$ if charging.

The control variables not only determine when to charge or discharge the battery storage, but also set the optimal operating conditions for charging and discharging.

5.5 Electricity Bill Optimization Algorithm

The following observations are the bases of the proposed offline optimization algorithm.

Observation 1: It is beneficial to charge the battery when the electricity is the cheapest, that is, time slot $n_{min} = \arg\min_n(C[n])$, and discharge the battery when the electricity is the most expensive, that is, $n_{max} = \arg\max_n(C[n])$.

Observation 2: Increasing the charging and discharging current of battery storage reduces the charging and discharging efficiency, respectively, due to the battery IR loss and the rate capacity effect.

From the aforesaid observations, it is beneficial to discharge the battery storage at time slot $n_{max} = \arg\max_n(C[n])$, but too much discharging would lower the benefit. We define the variable $C_{com}[n]$, that is the *compensated cost* for effectively determining the time and magnitude of charge/discharge current. Due to the non-ideal characteristics of the power converters and battery storage, charging and discharging efficiency is less than 100%. We reflect the non-ideal characteristics in the variable, $C_{com}[n]$, as follows. The value of $C_{com}[n]$ is initialized to $C[n]$ at the beginning of the algorithm, and it is updated according to the following equation in each iteration.

$$C_{com}[n] = \begin{cases} \dfrac{E_{supplied}}{E_{charge} - E_{loss}} \cdot C[n], & \text{when charging,} \\ \dfrac{E_{extracted}}{E_{extracted} + E_{loss}} \cdot C[n], & \text{when discharging,} \end{cases} \tag{5.7}$$

where $E_{supplied}$ and $E_{extracted}$ denote the amounts of electrical energy that is supplied to and extracted from the terminal of the battery. E_{loss} is the loss due to the battery IR loss and the rate capacity effect. Higher charging or discharging current makes E_{loss} higher. For example, suppose charging the battery from

the Grid at time slot $n_{min} = \arg\max_n(C_{com}[n])$. As our iterative algorithm increases the charging current gradually, $C_{com}[n_{min}]$ increases. As the charging current becomes too high, the compensated cost C_{com} will also become high, and thus further increasing the charging current is avoided. The same approach applies to discharging vice versa when the electricity price is high.

The solution to electricity bill minimization is composed of two parts. The first part of the solution involves solving the electricity bill minimization problem without the maximum battery capacity constraint as shown in Algorithm 2. It assumes that the battery capacity is unlimited. For practical cases, the size of battery is limited, often much smaller than the total load energy consumption throughout a day. Thus, the second part of the solution involves solving the problem with the battery capacity limit constraint based on the solution of the first part as shown in Algorithm 3.

- Operating condition τ : $(v_{bus}, P_{bus,pv}, P_{bus,b}, P_{bus,inv})$ pair that describes the operating condition of the system. The terms correspond to the voltage of the DC-bus, PV converter output power, input/output power to/from the battery charger/converter, and input/output powers of the inverter/rectifier, respectively.

- `VBUS_LUT_1`: lookup table of optimal v_{bus} for given G and I_{load} values constructed at offline.

- `VBUS_LUT_2`: lookup table of optimal v_{bus} for given discharging $P_{bus,b} > 0$ and I_{load} values constructed at offline.

- `VBUS_LUT_3`: lookup table of optimal v_{bus} for given charging $P_{bus,b} < 0$ and I_{load} values constructed at offline.

- `MPTT`: optimal PV operating point (V_{pv}, I_{pv}) for given G and v_{bus}.
- $P^{max}_{bus,pv}(G)$: the PV converter output power for given solar irradiance G and the optimal v_{bus}.
- $P^{min}_{bus,inv}(I_{load})$: the inverter input power when the I_{load} is supplied wholly by the inverter output for the optimal v_{bus}.
- n_s, n_e: the beginning of *active management period* defined by the time when $P^{max}_{bus,pv}$ becomes greater than $P^{min}_{bus,inv}(I_{load})$, and the end of *active management period* defined by 24 hours plus n_s.

Algorithm 2 determines the operating condition τ for every time slot. The power values $P_{bus,pv}$, $P_{bus,b}$, $P_{bus,inv}$ are defined on the DC-bus side of the converter. Three lookup tables `VBUS_LUT_1`, `VBUS_LUT_2`, and `VBUS_LUT_3` are built offline. They contain optimal values of v_{bus} that maximizes the actual power delivered from the source to destination considering the conversion losses. We obtain converter losses from the converter model, and thus, $V_{pv}[n]$, $I_{pv}[n]$, $I_b[n]$, etc. The key idea of Algorithm 2 is to use two threshold values, $c_{th,low}$ and $c_{th,high}$. We initialize the low threshold value to $min(C_{com}[n])$. If we pick all the time slots n with $C_{com}[n] = c_{th,low}$, these are the slots with minimum electricity cost, and thus, are suitable candidates for battery charging. Throughout the algorithm, $c_{th,low}$ gradually increases, as C_{com} increases. We initialize $c_{th,high}$ to $max(C_{com}[n])$, and find all the time slots n with $C_{com}[n] = c_{th,high}$, which are suitable for discharging the battery. We store the cheapest electricity in the battery and use it when the electricity price is the highest. Power from the PV array is free, and always cheaper than the Grid electricity price. The algorithm considers charging the battery with PV power first, and the electricity from the

Algorithm 2: Electricity bill minimzation algorithm without battery capacity limit.

Input: G: irradiance, I_{load}: load current
Output: Operating condition $\tau = (v_{bus}, P_{bus,pv}, P_{bus,b}, P_{bus,inv})$

for $\forall n,\ P^{max}_{bus,pv}(G[n]) > P^{min}_{bus,inv}(I_{load}[n])$ **do**
  $v_{bus}[n] \leftarrow \texttt{VBUS\_LUT\_1}(G[n], I_{load}[n])$
  $(V_{pv}[n], I_{pv}[n]) \leftarrow \texttt{MPTT}(G[n], v_{bus}[n])$
  $P_{bus,pv}[n] \leftarrow V_{pv} \cdot I_{pv} \cdot \eta^{in}_{pv}(V_{pv}[n], v_{bus}[n], I_{pv}[n])$
  $P_{bus,inv}[n] \leftarrow \dfrac{V_{load} \cdot I_{load}[n]}{\eta^{out}_{inv}(v_{bus}[n], V_{load}, I_{load}[n])}$
  $P_{bus,b}[n] \leftarrow P_{bus,inv}[n] - P_{bus,pv}[n]$
  $P_b[n] \leftarrow \eta^{in}_b(V_{bus}[n], V_b, -P_{bus,b}[n]/V_{bus}[n])$
  $SOC_b \leftarrow charge(P_b, SOC_b)$
while $c_{th,low} < c_{th,high}$ && $!endCond$ **do**
  for $\forall n,\ C_{com}[n] = c_{th,high}$ **do**
    if $n = \phi$ **then**
      $c_{th,high} \leftarrow max(C_{com})$
      continue
    $P_{bus,b}[n] = min(P_{bus,b}[n] + P_{inc,d}, \dfrac{P_{load}[n]}{\eta^{out}_{inv}})$
    $v_{bus}[n] \leftarrow \texttt{VBUS\_LUT\_2}(P_{bus,b}[n], I_{load}[n])$
    $(V_{pv}[n], I_{pv}[n]) \leftarrow \texttt{MPTT}(G[n], v_{bus}[n])$
    $P_{bus,pv}[n] \leftarrow V_{pv} \cdot I_{pv} \cdot \eta^{in}_{pv}(V_{pv}[n], v_{bus}[n], I_{pv}[n])$
    $P_{bus,inv}[n] \leftarrow P_{bus,pv}[n] + P_{bus,b}$
    $P_b[n] \leftarrow \eta^{out}_b(V_b, V_{bus}[n], P_{bus,b}[n]/V_{bus}[n])$
    $SOC_b \leftarrow discharge(P_b, SOC_b)$
    $C_{com}[n] \leftarrow decreaseCost(P_{bus,b}$
    if $SOC_b = 0$ **then**
      break
  for $\forall n,\ C_{com}[n] = c_{th,low}$ **do**
    if $n = \phi$ **then**
      $c_{th,low} \leftarrow min(C_{com})$
      continue
    $P_{bus,b}[n] \leftarrow P_{bus,b}[n] - P_{inc,c}$
    $v_{bus}[n] \leftarrow \texttt{VBUS\_LUT\_3}(P_{bus,b}[n], I_{load}[n])$
    $(V_{pv}[n], I_{pv}[n]) \leftarrow \texttt{MPTT}(G[n], v_{bus}[n])$
    $P_{bus,pv}[n] \leftarrow V_{pv} \cdot I_{pv} \cdot \eta^{in}_{pv}(V_{pv}[n], v_{bus}[n], I_{pv}[n])$
    $P_{bus,inv}[n] \leftarrow P_{bus,pv}[n] + P_{bus,b}$
    $P_b[n] \leftarrow \eta^{in}_b(V_{bus}[n], V_b, -P_{bus,b}[n]/V_{bus}[n])$
    $SOC_b \leftarrow charge(P_b, SOC_b)$
    $C_{com} \leftarrow increaseCost(P_{bus,b})$
return $\tau \leftarrow (v_{bus}, P_{bus,pv}, P_{bus,b}, P_{bus,inv})$

Grid next. Algorithm 2 is optimal if the battery capacity is unlimited and the

Algorithm 3: Electricity bill minimzation algorithm with battery capacity limit $SOC_{b,max}$.

Input: G: irradiance, I_{load}: load current, $SOC_{b,init}$: initial SOC at n_s, $\tau = (v_{bus}, P_{bus,pv}, P_{bus,b}, P_{bus,inv})$: result of Algorithm 2
Output: Operating condition $(v_{bus}, P_{bus,pv}, P_{bus,b}, P_{bus,inv})$

```
1  n_{mark,s} ← n_s
2  n_{mark,e} ← n_s
3  SOC_mark ← SOC_{b,init}
4  for n = n_s to n_e do
5      SOC_b ← updateSOC(P_{bus,b}[n], SOC_b)
6      if SOC_b > SOC_{b,max} then
7          n_{mark,e} ← nextDischarge(P_{bus,b}, n)
8          τ[n] ← reschedule1(SOC_mark, SOC_{b,max}, n_{mark,s}, n_{mark,e})
9          n_{mark,s} ← n_{mark,e}
10         SOC_mark ← SOC_{b,max}
11         continue
12     else if SOC_b < 0 then
13         n_{mark,e} ← nextCharge(P_{bus,b}, n)
14         τ[n] ← reschedule2(SOC_mark, 0, n_{mark,s}, n_{mark,e})
15         n_{mark,s} ← n_{mark,e}
16         SOC_mark ← 0
17         continue
18 return τ ← (v_bus, P_{bus,pv}, P_{bus,b}, P_{bus,inv})
```

initial state of charge (SOC) of battery is sufficient.

Algorithm 3 reschedules the battery charging and discharging operations so that the battery SOC does not exceed the maximum value or becomes below zero. The charging and discharging schedule from Algorithm 2 might violate both the maximum and minimum battery capacity constraint. Algorithm 3 starts at the beginning of a *active management period*, n_s. Algorithm 3 charges and discharges the battery according to the scheduling result of Algorithm 2 as time passes until the battery capacity constraint is violated. Functions $nextDischarge(P_{bus,b}, n)$ and $nextCharge(P_{bus,b}, n)$ find the

timeslot next to n where the closest discharge or charge begins. The functions $reschedule1()$ and $reschedule2()$ derive an operating condition τ schedule that makes SOC_b from SOC_{mark} to $SOC_{b,max}$ and from $SOC_{mark}$to 0 during time interval $[n_{mark,s}\ n_{mark,e}]$, respectively, while meeting the battery capacity constraints. This rescheduling problem is much simpler than the original problem since the start and end SOC values are given, and the capacity limit is met for the interval $[n_{mark,s}\ n_{mark,e}]$. Function $reschedule1()$ works as follows. It fixes the discharging schedule as derived in Algorithm 2. The next step is to perform initial charging to avoid depletion by the discharging schedule fixed in the previous step. This initial charging is always feasible from the definition of the interval $[n_{mark,s}\ n_{mark,e}]$. Finally, $reschedule1()$ determines the rest of the charging schedule using $c_{th,low}$ and C_{com} to minimize the charging cost until the total accumulated charge at $n_{mark,e}$ becomes $SOC_{b,max}$. Function $reschedule2()$ is defined in a complementary manner. Algorithm 3 is based on Algorithm 2 and ensures the solution quality of the capacity limited problem because Algorithm 2 gives the optimal results for the unconstrained case.

5.6 Experiments

We compare the efficacy of the proposed algorithm with two baseline algorithms on various EV charging scenarios. Both baseline algorithms charge the battery from the PV array and Grid during off-peak hours and discharge the battery during the peak hours. For the first baseline, charging and discharging current from the Grid is fixed to 1C to maximize cycle efficiency of the battery, and it performs MPTT to determine the operating point of the PV array and DC-bus voltage. For the second baseline, the charging current from the Grid is fixed to

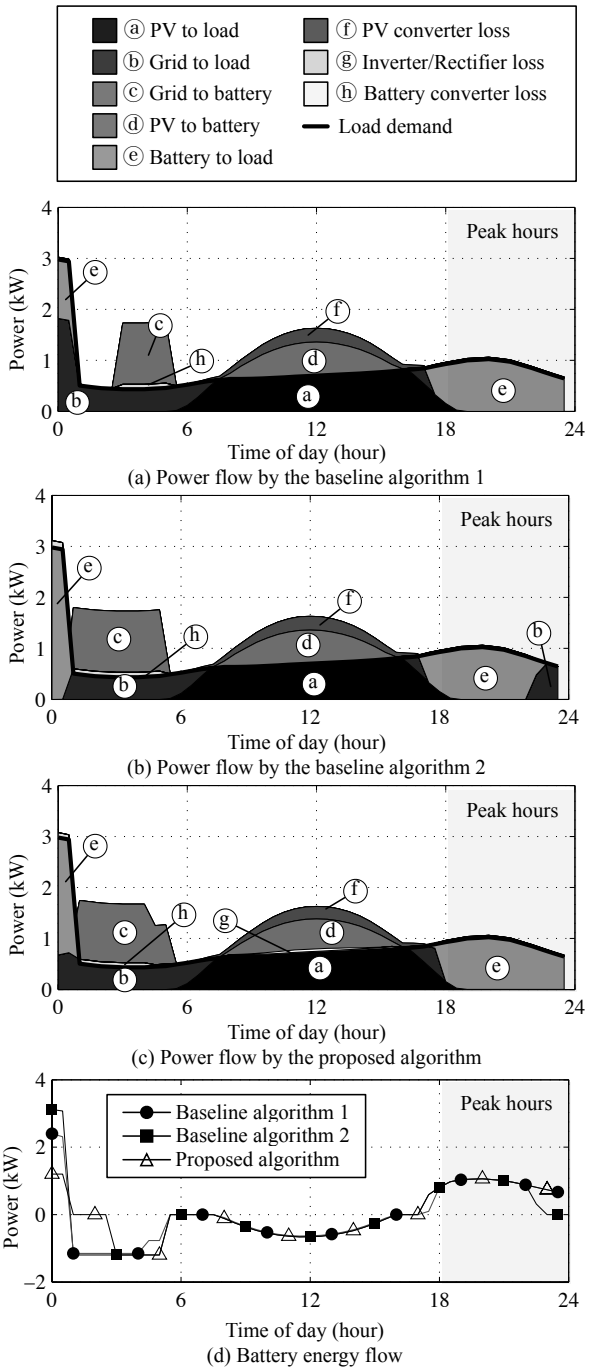

Figure 5.4 Power input and output variation with time for level 1 charging of Prius sized battery.

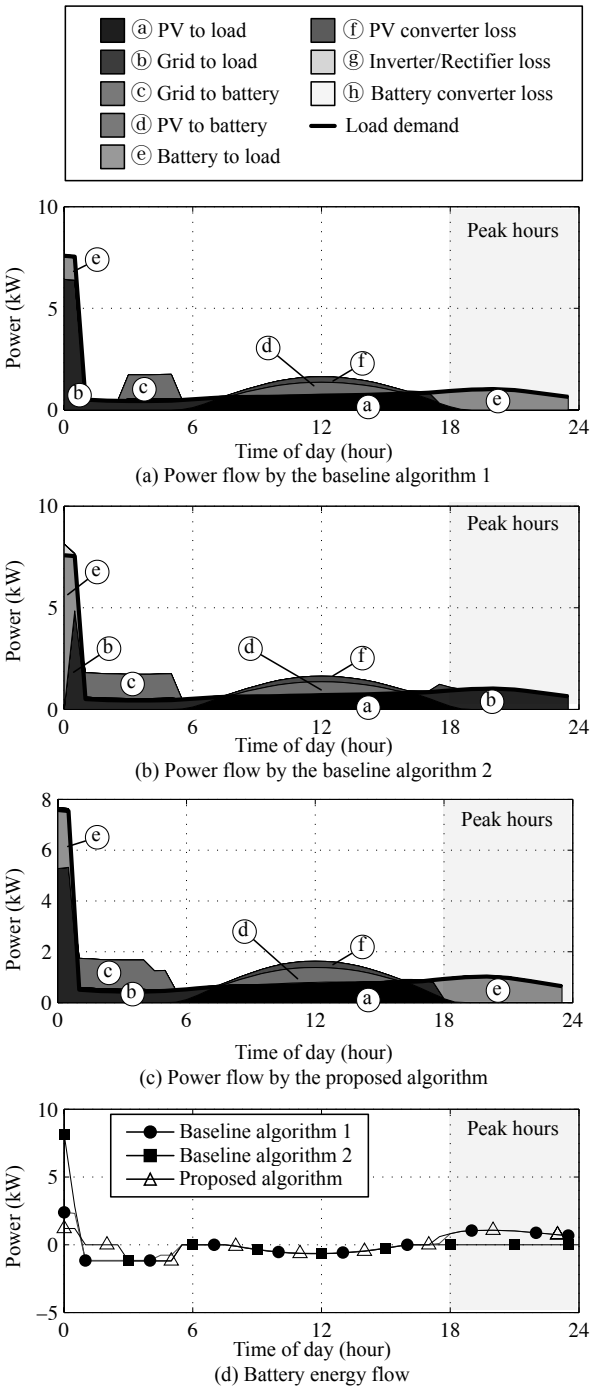

Figure 5.5 Power input and output variation with time level 2 charging of Prius sized battery.

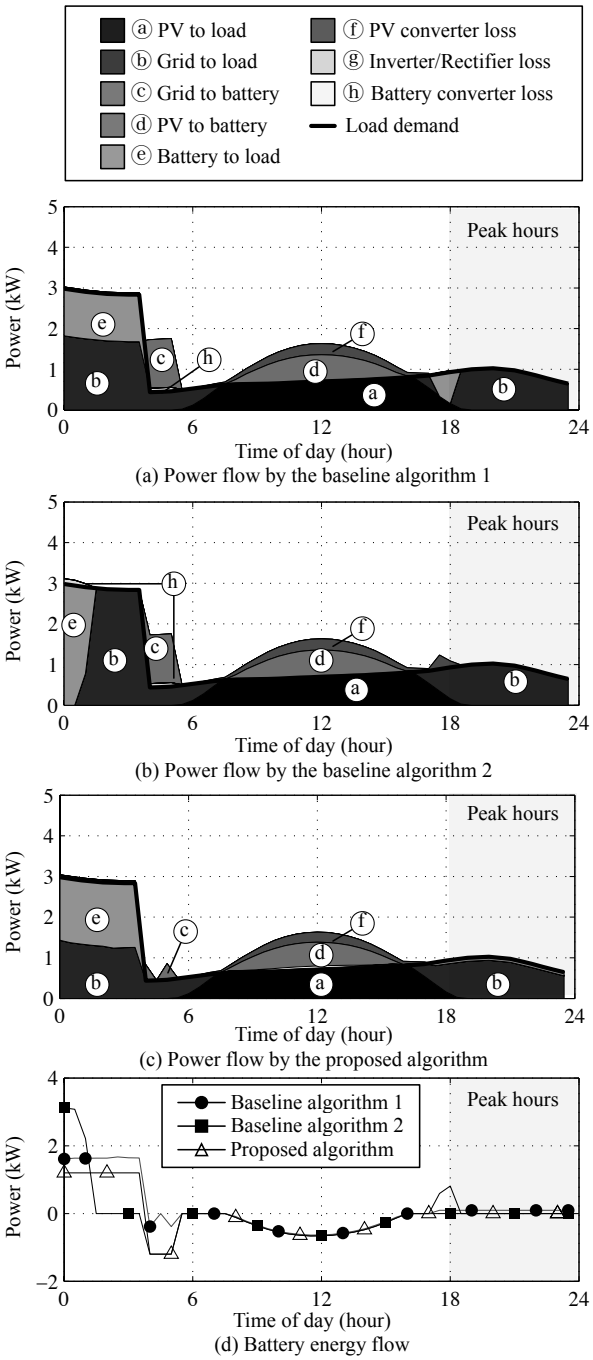

Figure 5.6 Power input and output variation with time level 1 charging of Nissan Leaf sized battery.

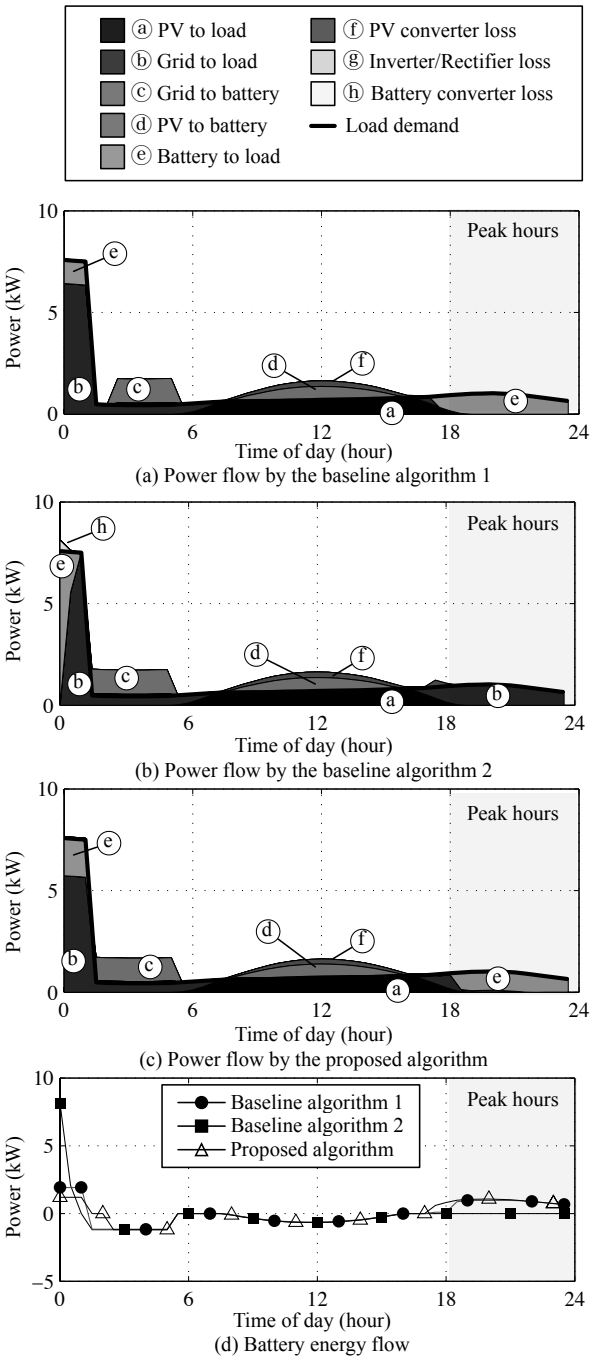

Figure 5.7 Power input and output variation with time level 2 charging of Nissan Leaf sized battery.

1C and discharging current is determined greedily during the peak hours, and it also performs MPTT.

We use an actual profile of residential load demand and Grid electricity price from Southern California [34, 2]. The peak load demand is 1.025 kW at 8pm as shown in Figure 5.2. The unit price of the Grid electricity is 23.77 ¢/kWh during peak hours and 12.37 ¢/kWh during off-peak hours. The PV array used for our experiment outputs 1,000 W/m^2 and the maximum power point voltage and current is 67.8 V and 23.6 A. The capacity of battery bank is 12 kWh rated at 12.5 A output current with the output voltage of 96 V.

We consider four EV charging scenarios. First is level 1 charging of Toyota Prius Plug-in Hybrid sized (4.4 kWh) EV battery. Second one is level 2 charging of Toyota Prius Plug-in Hybrid sized EV battery. Third one is level 1 charging of Nissan Leaf sized (24 kWh) EV battery. Fourth one is level 2 charging of Nissan Leaf sized EV battery. Each scenarios differ in peak power and total energy required for charging the EVs.

The resulting battery management policy shows different charging and discharging patterns. Results for Level 1 charging of Toyota Prius Plug-in Hybrid is shown in Figure 5.4. Level 1 charging charges EV battery at around 2.4 kWh, which sums up with other residential load demand to around 3 kWh from midnight. The electricity bills for each policy are 63 cents/day, 65 cents/day, and 62 cents/day, respectively, for the first scenario. Baseline algorithm 1 limits the residential battery discharge rate, such that there is significant electricity usage from the power grid as shown in Figure 5.4(a). Limiting the maximum battery discharge rate limits further gain because the net energy into and out of the battery should be zero during a day according to our assumptions. Baseline

algorithm 2 performs greedy discharge such that almost all of the EV battery charging power is supported by the residential battery as shown in Figure 5.4(b). However, this causes more loss in the conversion circuitry and forces that more grid power to be used during the peak hours. The proposed algorithm finds the optimal residential battery discharge current and maximizes the user benefits by balancing the amount of power from the residential battery and the grid. Discharging the battery at higher current than Baseline 1 increases the rate capacity loss, but it is beneficial due to the price difference between the peak and off-peak hours and grid price increase due to high EV charging power. The proposed algorithm determines the charging and discharging schedule while considering both the loss due to large charge/discharge current and utilization of the Grid price fluctuation.

Results for Level 2 charging of Toyota Prius Plug-in Hybrid is shown in Figure 5.4. The electricity bills for three policies are 125 cents/day, 157 cents/day, and 121 cents/day, respectively. Level 2 charging provides higher EV charging power and shorter time for charging the EV battery of same capacity. The result is more distinguishable compared with the first scenario as the discharging current is high and rate capacity effect plays a more important role. Baseline algorithm 1 exhibits slightly higher electricity bill compared with the proposed algorithm due to the same reason as the first scenario. Baseline algorithm 2 is unable to utilize the residential battery energy during the peak hours because all of the energy is used for charging the EV battery. It greedily discharges the battery for charging the EV battery, and there is no other choice but to use expensive Grid electricity beyond that point, which increases the electricity bill. The proposed algorithms successfully balances this situation and utilizes

the energy stored in residential battery effectively both to supply the power to the residential load and to charge the EV battery.

Results for Level 1 charging of Nissan Leaf is shown in Figure 5.6. The charging power is the same as the first scenario, but larger EV battery size requires longer time to charge it. The electricity bills for each policy are 174 cents/day, 193 cents/day, and 143 cents/day, respecitvely. The analysis for the trend is almost the same as the first two scenarios. However, the gain of the proposed algorithms is larger because the effect of increased grid electricity price due to high EV charging is dominant in the scenario.

Results for Level 2 charging of Nissan Leaf is shown in Figure 5.7. The electricity bills for each policy is 171 cents/day, 207 cents/day, and 159 cents/day. It poses the largest burden to the residential PV system due to its high power requirement and large energy required for charging the EV battery. The capacity and power demand of this scenarios is different, and we have verified that the proposed algorithm is still effective in reducing the electricity bill.

5.7 Summary

PV power generation is promising but not very effective to mitigate demand and supply mismatch of electricity. Grid-connected PV systems with a battery has great potential to resolve the mismatch as long as elaborated battery management ensures optimal charge and discharge policies. PV power is efficient for charging the EV batteries as it is free of carbon emission during operation unlike grid power, which is often generated from dirty power sources. In this chapter, we addressed holistic optimization of battery management for Grid-connected PV systems with an EV. We devise an offline algorithm that schedules battery

charge and discharge for solar given solar irradiance, residential load profile and EV charging scenario. Our framework allows for arbitrary Grid electricity price function, and all the lossy components, such as converter loss, and rate capacity loss of batteries, in the Grid-connected PV powered system with electrical energy storage. Experimental results show that the electricity price is reduced significantly when compared with baseline policies for various EV charging scenarios.

Chapter 6

Electric Vehicle HESS Implementation

6.1 EV Prototype

6.1.1 Design Specifications

We build a prototype EV, which features 3 kW output power with weight of 300 kg. Detailed specifications of the prototype EV is described in Table 6.1. The front-wheel drive system complicates the mechanical design as it requires constant velocity joints and tie rod, but it is essential in EV prototype because braking torque is concentrated to the front wheel. As regenerative braking energy is available only on wheels with motors, the architecture directly relates to the energy efficiency of the vehicle. It consists of battery-supercapacitor HESS with a custom-designed charger, two inverters, two BLDC motors.

Figure 6.1 Prototype EV frame with traction motors, steering and suspension system assembled.

Table 6.1 Specifications of the EV prototype.

Item	Value
Layout	Front-motor, front-wheel drive
Electric motor	Two 1.5 kW synchronous motor (4.023 hp)
Maximum speed	30.2 km/h
Axle ratio	single speed constant ratio (7:1)
Battery	1.44 kWh Li-polymer battery
Supercapacitor	11.6 F, 84 V (11.35 Wh)
Wheelbase	1,200 mm
Length	1,700 mm
Width	1,700 mm
Weight	300 kg

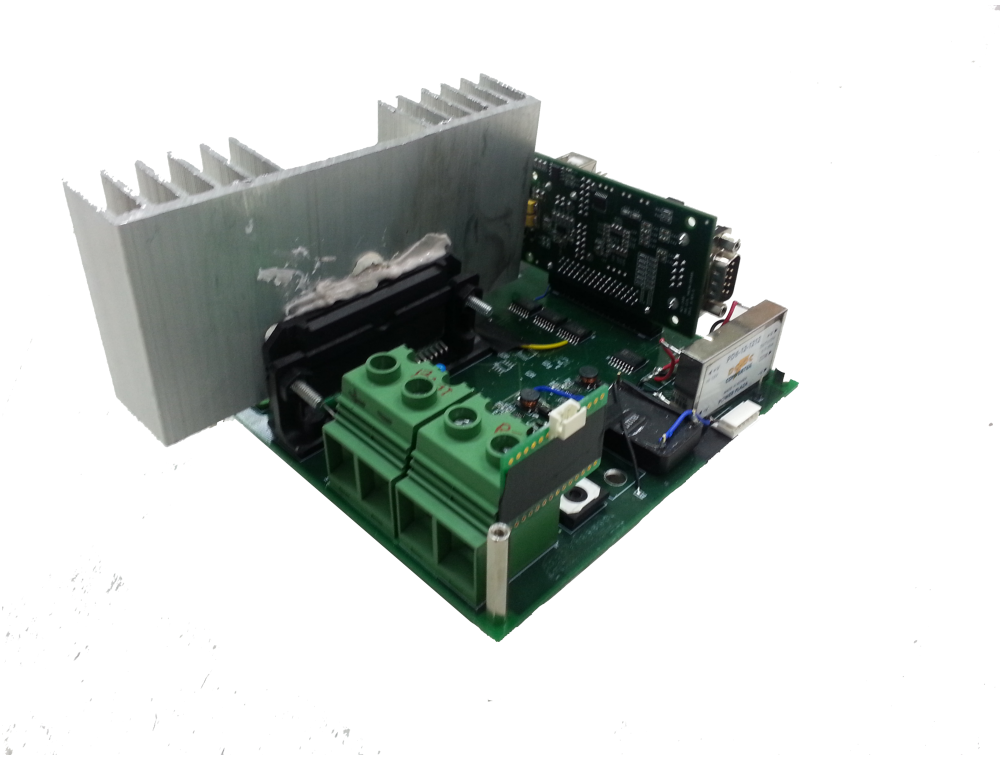

Figure 6.2 Motor driver based on STK-621-061-E 3-phase bridge and TI Stellaris LM3S microcontroller.

6.1.2 Motor Driver Design

We developed a custom designed motor driver based on IGBTs (insulated-gate bipolar transistor) shown in Figure 6.2. The custom designed motor driver offers full degree of freedom in controlling the 3-phase bridge, so that we can test various techniques for efficiency enhancement of motor drive and regenerative braking of the EV motors. IGBTs have advantages over MOSFETs in situations where supply voltage is high, and the switching frequency is low. The characteristics make IGBTs suitable for EV motor driver applications. The motor driver is based on STK-621-061-E from ON Semiconductor, in which a 3-phase bridge, gate drivers, and bootstrap circuit is included. The internal gate driver and bootstrap circuit greatly simplifies the driver design as it relieves the burden of external high-side gate drive circuit. Electrically isolated TI Stellaris LM3S microcontroller (LM3S2965) controls of the PWM gate drive signals.

6.1.3 Motor and Gearbox

The EV prototype uses two 3-phase BLDC motors attached to each front wheel. The motors are custom-designed by TM Tech-I Inc. to meet the EV specifications. The motors receive 3-phase 72 VDC, exhibit maximum power of 1.5 kW each, maximum 2,000 RPM, nominal torque of 7.17 N·m, and instantaneous torque of 14.34 N·m. EV traction motors generally require a gearbox to increase torque with reduced RPM. We use a gearbox with ratio of 7:1 to provide sufficient torque for the vehicle to climb a slope of up to 5°. The maximum vehicle speed is 30 km/h at 2,000 RPM.

(a) (b)

Figure 6.3 HESS storage elements. (a) Li-polymer battery pack 24 V/20 Ah. (b) Supercapacitor module 58 F/16.8 V from LS Mtron.

6.1.4 HESS

The HESS architecture is essentially similar to two-motor prototype. Instead, the capacity of the comprising elements is larger to support two 1.5 kW traction motors. Each Li-polymer battery pack is 24 V, 20 Ah capacity and contains protected cells inside. We stack three packs to obtain 72 V. Supercapacitor module capacitance is 58 F with maximum voltage of 16.8 V. We build 5S1P connection to build a bank of 11.6 F, 84 V supercapacitor bank. The capacity supercapacitor bank, 11.35 Wh, is definitely enough to provide and receive one time vehicle acceleration and deceleration energy $\frac{1}{2} \cdot 400 \text{ kg} \cdot (30.2 \text{ km/h})^2 = 3.91$ Wh with 100 kg load.

6.1.5 System Monitoring subsystem

An EV requires several monitoring points such as voltage/current of the ESS elements, input/output voltage of the motor driver and chargers, temperature

of the battery bank, and motors, slope of the road, geographical location, and ambient air temperature, and so on. We build a sensor monitoring system based on CAN (controller area network) bus. Atmel 8-bit MCU, AT90CAN128, in each enclosure gather the output data of various sensors, and sends them to a monitoring module via CAN bus.

Chapter 7

Conclusions

Energy storage systems (ESS) of electric vehicles (EV) still require much effort in design and runtime algorithms to make them more commercially competitive to traditional vehicles. Energy efficiency enhancement is one of the most demanding requirements to make EV commercially competitive. There are many ways to enhance EV energy efficiency, especially for electricity generation, transmission and conversion, which are major power loss. However, they are not only related to EV development but nation-wide infrastructure renovation.

This dissertation reviews various aspects of EVs to maximize the energy efficiency and user benefits. First, the concept of maximum power transfer tracking (MPTT) has been introduced for regenerative braking. Usage of battery-supercapacitor HESS and performing MPTT enhances the energy efficiency of regenerative braking. Second, proactive charge migration among ESS banks during stopping/cruising enables energy efficiency enhancement. Systematic en-

hancement of regenerative braking efficiency for hybrid energy storage systems (HESS) in EV. Energy efficiency enhancement of the regenerative braking gives significant impact on carbon emission because it is energy harvesting directly from the wheels to EV HESS unlike plugin charging from the grid electricity coming from fuel through power plant, transformers, transmission lines, and distribution lines. The proposed method decouples ESS charging efficiency optimization from the supercapacitor state of charge (SoC) management, which generally sacrifices the charging efficiency in previous works due to the limited supercapacitor capacitance. Third, an optimization algorithm to minimize the electricity bill in residential photovoltaic installation has been proposed. This, in turn, minimizes the cost per mile of the EV owner and maximize the EV cost of ownership. Fourth, we implement an actual EV prototype equipped with HESS to show the validity of the approach. I conclude this dissertation by stating that adopting HESS design methodology improves EV in various aspects, and there still remains much research to do.

- Best EV charging infrastructure from the grid perspective
- Charge scheduling of charging stations, which serves a number of EVs
- EV ESS design to minimize the capital cost of a EV

Bibliography

[1] *NEDC, European Council Directive, 70/220/EEC with amendments.*

[2] Review of residential electrical energy use data. Technical report, NAHB Research Center, Inc., 2001.

[3] MOSFET power losses calculation using the data-sheet parameters. Technical report, Infineon, 2006.

[4] U.S. solar market trends, 2010. Technical report, Interstate Renewable Energy Council, 2011.

[5] ABB Inc. Energy efficiency in the power grid. 2007.

[6] D. Aggeler, F. Canales, H. Zelaya-De La Parra, A. Coccia, N. Butcher, and O. Apeldoorn. Ultra-fast dc-charge infrastructures for ev-mobility and future smart grids. In *Innovative Smart Grid Technologies Conference Europe (ISGT Europe), 2010 IEEE PES*, pages 1–8, 2010.

[7] P. Arun, R. Banerjee, and S. Bandyopadhyay. Optimum sizing of photovoltaic battery systems incorporating uncertainty through design space approach. *Solar Energy*, 83(7):1013–1025, 2009.

[8] H. Bai and C. Mi. The impact of bidirectional dc-dc converter on the inverter operation and battery current in hybrid electric vehicles. In *Power Electronics and ECCE Asia (ICPE ECCE), 2011 IEEE 8th International Conference on*, pages 1013–1015, 2011.

[9] A. Bazzi. Electric machines and energy storage technologies in evs and hevs for over a century. In *Electric Machines Drives Conference (IEMDC), 2013 IEEE International*, pages 212–219, 2013.

[10] D. K. Bellman. Power plant efficiency outlook. In *Working Document of the NPC Global Oil & Gas Study*, 2007.

[11] J. Cao and A. Emadi. A new battery/ultracapacitor hybrid energy storage system for electric, hybrid, and plug-in hybrid electric vehicles. *IEEE T. on Power Electronics*, 2012.

[12] R. Carter and A. Cruden. Strategies for control of a battery/supercapacitor system in an electric vehicle. In *Proc. of SPEEDAM*, 2008.

[13] S. Chakraborty, M. Lukasiewycz, C. Buckl, S. Fahmy, N. Chang, S. Park, Y. Kim, P. Leteinturier, and H. Adlkofer. Embedded systems and software challenges in electric vehicles. In *Proc. of DATE*, 2012.

[14] S. Chiang, K. Chang, and C. Yen. Residential photovoltaic energy storage system. *Industrial Electronics, IEEE Transactions on*, 45(3):385–394, 1998.

[15] Y. Choi, N. Chang, and T. Kim. DC-DC converter-aware power management for low-power embedded systems. *IEEE T. on CAD*, 2007.

[16] K. Clement-Nyns, E. Haesen, and J. Driesen. The impact of charging plug-in hybrid electric vehicles on a residential distribution grid. *Power Systems, IEEE Transactions on*, 25(1):371–380, 2010.

[17] J. Dixon, M. Ortuzar, and E. Wiechmann. Regenerative braking for an electric vehicle using ultracapacitors and a buck-boost converter. In *EVS*, 2000.

[18] M. Dubarry, C. Truchot, M. Cugnet, B. Y. Liaw, K. Gering, S. Sazhin, D. Jamison, and C. Michelbacher. Evaluation of commercial lithium-ion cells based on composite positive electrode for plug-in hybrid electric vehicle applications. part I: Initial characterizations. *J. of Power Sources*, 2011.

[19] B. Eberleh and T. Hartkopf. A high speed induction machine with two-speed transmission as drive for electric vehicles. In *Power Electronics, Electrical Drives, Automation and Motion, 2006. SPEEDAM 2006. International Symposium on*, pages 249–254, 2006.

[20] A. Emadi, Y.-J. Lee, and K. Rajashekara. Power electronics and motor drives in electric, hybrid electric, and plug-in hybrid electric vehicles. *Industrial Electronics, IEEE Transactions on*, 55(6):2237–2245, 2008.

[21] Environmental Protectino Agency and US Department of Energy. Greenhouse gas emissions for electric and plug-in hybrid electric vehicles. In *www.fueleconomy.com*, 2012.

[22] T. Esram, J. Kimball, P. Krein, P. Chapman, and P. Midya. Dynamic maximum power point tracking of photovoltaic arrays using ripple correlation control. *Power Electronics, IEEE Transactions on*, 21(5):1282–1291, 2006.

[23] E. Evarts. Leaf, volt tests show electric cars cost else per mile to operate. In *Consumer Reports News*, 2011.

[24] Forward, E. and Glitman, K. and Roberts, D. *An Assessment of Level 1 and Level 2 Electric Vehicle Charging Efficiency*, 2013.

[25] F. Giraud and Z. Salameh. Steady-state performance of a grid-connected rooftop hybrid wind-photovoltaic power system with battery storage. *Energy Conversion, IEEE Transactions on*, 16(1):1–7, 2001.

[26] S. Govindan, A. Sivasubramaniam, and B. Urgaonkar. Benefits and limitations of tapping into stored energy for datacenters. In *Proceedings of the 38th annual international symposium on Computer architecture*, ISCA '11, pages 341–352, New York, NY, USA, 2011. ACM.

[27] Y. Gurkaynak and A. Khaligh. Control and power management of a grid connected residential photovoltaic system with plug-in hybrid electric vehicle (PHEV) load. In *Applied Power Electronics Conference and Exposition*, pages 2086–2091, 2009.

[28] G. Joos, M. De Freige, and M. Dubois. Design and simulation of a fast charging station for phev/ev batteries. In *Electric Power and Energy Conference (EPEC), 2010 IEEE*, pages 1–5, 2010.

[29] Y. Kim, S. Park, Q. Xie, Y. Wang, N. Chang, and M. Pedram. Networked architecture for hybrid electrical energy storage systems. In *Proceedings of Proceedings of the Design Automation Conference (DAC)*, pages 522–528, June 2012.

[30] Y. Kim, Y. Wang, N. Chang, and M. Pedram. Maximum power transfer tracking for a photovoltaic-supercapacitor energy system. In *Proc. of ISLPED*, 2010.

[31] J. Kolar, H. Ertl, and F. Zach. Influence of the modulation method on the conduction and switching losses of a pwm converter system. *Industry Applications, IEEE Transactions on*, 27(6):1063–1075, 1991.

[32] J. Lai, R. Young, and J. McKeever. Efficiency consideration of dc link soft-switching inverters for motor drive applications. In *Power Electronics Specialists Conference, PESC'94 Record., 25th Annual IEEE*, pages 1003–1010. IEEE, 1994.

[33] W. Lee, Y. Wang, D. Shin, N. Chang, and M. Pedram. Power conversion efficiency characterization and optimization for smartphones. In *Proceedings of IEEE/ACM International Symposium on Low Power Electronics and Design (ISLPED)*, pages 103–108, August 2012.

[34] Los Angeles Department of Water & Power. *Electric Rates, http://www.ladwp.com/ladwp/cms/ladwp001752.jsp*, 2009.

[35] B. Lu and M. Shahidehpour. Short-term scheduling of battery in a grid-connected pv/battery system. *Power Systems, IEEE Transactions on*, 20(2):1053–1061, 2005.

[36] S. Lukic, S. Wirasingha, F. Rodriguez, J. Cao, and A. Emadi. Power management of an ultracapacitor/battery hybrid energy storage system in an hev. In *IEEE VPPC*, 2006.

[37] K. Mets, T. Verschueren, W. Haerick, C. Develder, and F. De Turck. Optimizing smart energy control strategies for plug-in hybrid electric vehicle charging. In *Network Operations and Management Symposium Workshops (NOMS Wksps), 2010 IEEE/IFIP*, pages 293–299, 2010.

[38] K. Morrow, D. Karner, and J. Francfort. Plug-in hybrid electric vehicle charging infrastructure review. *US Department of Energy Vehicle Technologies Program – Advanced Vehicle Testing Activity*, 2008.

[39] N. Omar, M. Daowd, P. v. d. Bossche, O. Hegazy, J. Smekens, T. Coosemans, and J. v. Mierlo. Rechargeable energy storage systems for plug-in hybrid electric vehiclesâ assessment of electrical characteristics. *Energies*, 5(8):2952–2988, 2012.

[40] M. Ortuzar, J. Moreno, and J. Dixon. Ultracapacitor-based auxiliary energy system for an electric vehicle: Implementation and evaluation. *IEEE T. on Industrial Electronics*, 2007.

[41] G. Palomino, J. Wiles, J. Stevens, and F. Goodman. Performance of a grid connected residential photovoltaic system with energy storage. In *Photovoltaic Specialists Conference*, pages 1377–1380, 1997.

[42] M. Park, S. Kim, L. Yang, and K. Kim. Development of the control logic of electronically controlled hydraulic brake system for hybrid vehicle. In *SAE World Congress*, 2009.

[43] M. Pedram, N. Chang, Y. Kim, and Y. Wang. Hybrid electrical energy storage systems. In *Proc. of ISLPED*, 2010.

[44] S. B. Peterson, J. Whitacre, and J. Apt. The economics of using plug-in hybrid electric vehicle battery packs for grid storage. *J. of Power Sources*, 2010.

[45] K. Qian, C. Zhou, M. Allan, and Y. Yuan. Modeling of load demand due to ev battery charging in distribution systems. *Power Systems, IEEE Transactions on*, 26(2):802–810, 2011.

[46] A. D. Rajapakse, A. M. Gole, and P. L. Wilson. Approximate loss formulae for estimation of igbt switching losses through emtp-type simulations. In *International Conference on Power Systems Transients (IPST)*, 2005.

[47] D. Rakhmatov. Battery voltage modeling for portable systems. *Design Automation of Electronic Systems, ACM Transactions on*, 2009.

[48] M. Ramsey. Nissan says leaf electric will be profitable with u.s. plant. In *The Wall Street Journal*, 2010.

[49] E. Rask, T. Bohn, and K. Gallagher. On charging equipment and batteries in plug-in vehicles: Present status. In *Proceedings of the 2012 IEEE PES Innovative Smart Grid Technologies*, page 1. IEEE Computer Society, 2012.

[50] P. Rong and M. Pedram. An analytical model for predicting the remaining battery capacity of lithium-ion batteries. *Very Large Scale Integration (VLSI) Systems, IEEE Transactions on*, 14(5):441–451, 2006.

[51] N. Rotering and M. Ilic. Optimal charge control of plug-in hybrid electric vehicles in deregulated electricity markets. *Power Systems, IEEE Transactions on*, 26(3):1021–1029, 2011.

[52] E. Schaltz, A. Khaligh, and P. Rasmussen. Influence of battery/ultracapacitor energy-storage sizing on battery lifetime in a fuel cell hybrid electric vehicle. *IEEE T. on Vehicular Technology*, 2009.

[53] S. Shaahid and I. El-Amin. Techno-economic evaluation of off-grid hybrid photovoltaic-diesel-battery power systems for rural electrification in saudi arabia—a way forward for sustainable development. *Renewable and Sustainable Energy Reviews*, 13(3):625–633, 2009.

[54] D. Shin, Y. Kim, Y. Wang, N. Chang, and M. Pedram. Constant-current regulator-based battery-supercapacitor hybrid architecture for high-rate pulsed load applications. *Journal of Power Sources (JPS)*, 205:516–524, May 2012.

[55] D. Shin, Y. Wang, Y. Kim, J. Seo, N. Chang, and M. Pedram. Battery-supercapacitor hybrid system for high-rate pulsed load applications. In *Proc. of DATE*, 2011.

[56] A. Shumway-Cook and M. H. Woollacott. *Motor control: theory and practical applications*, volume 157. Williams & Wilkins Baltimore:, 1995.

[57] A. Tashakori, M. Ektesabi, and N. Hosseinzadeh. Modeling of bldc motor with ideal back-emf for automotive applications. In *in Proc. WCE*, 2011.

[58] C. S. Thomas. Transportation options in a carbon-constrained world: Hybrids, plug-in hybrids, biofuels, fuel cell electric vehicles, and battery electric vehicles. *International Journal of Hydrogen Energy*, 34(23):9279 – 9296, 2009.

[59] US Department of Energy, Energy Efficiency and Renewable Energy. Improving motor and drive system performance: A sourcebook for industry. 2008.

[60] US Energy Information Adminstration. State electricity profiles. In *http://www.eia.gov/electricity/state/*, 2013.

[61] M. Villalva, J. Gazoli, and E. Filho. Comprehensive approach to modeling and simulation of photovoltaic arrays. *Power Electronics, IEEE Transactions on*, 24(5):1198–1208, 2009.

[62] R. Wang, Y. Chen, D. Feng, X. Huang, and J. Wang. Development and performance characterization of an electric ground vehicle with independently actuated in-wheel motors. *Journal of Power Sources*, 196(8):3962 – 3971, 2011.

[63] Y. Wang, Y. Kim, Q. Xie, N. Chang, and M. Pedram. Charge migration efficiency optimization in hybrid electrical energy storage (HEES) systems. In *Proc. of ISLPED*, 2011.

[64] Y. Wang, Q. Xie, M. Pedram, Y. Kim, N. Chang, and M. Poncino. Multiple-source and multiple-destination charge migration in hybrid electrical energy storage systems. In *Proc. of DATE*, 2012.

[65] S. Williamson, A. Emadi, and K. Rajashekara. Comprehensive efficiency modeling of electric traction motor drives for hybrid electric vehicle propulsion applications. *Vehicular Technology, IEEE Transactions on*, 56(4):1561–1572, 2007.

[66] S. Williamson, S. Lukic, and A. Emadi. Comprehensive drive train efficiency analysis of hybrid electric and fuel cell vehicles based on motor-controller efficiency modeling. *Power Electronics, IEEE Transactions on*, 21(3):730–740, 2006.

[67] J. Y. Wong. *Theory of ground vehicles*. Wiley-Interscience, 2001.

[68] Q. Xie, Y. Wang, Y. Kim, N. Chang, and M. Pedram. Charge allocation for hybrid electrical energy storage systems. In *Proc. of CODES+ISSS*, 2011.

[69] Q. Xie, Y. Wang, Y. Kim, D. Shin, N. Chang, and M. Pedram. Charge replacement in hybrid electrical energy storage systems. In *Proc. of ASP-DAC*, 2012.

[70] H. Yeo, D. Kim, S. Hwang, and H. Kim. Regenerative braking algorithm for a HEV with CVT ratio control during deceleration. In *Proc. of SAE CVT Congress*, 2004.

요약

전기자동차는 연비, 에너지 효율, 환경에의 영향 등의 측면에서 엔진 기반의 기존 차량에 강점을 가지며 이를 대체할 수 있으리라 기대되고 있다. 그러나 전기자동차의 실제 장점을 명확하게 조사한 연구는 많지 않으며, 특히 전기차의 에너지 저장장치(ESS)의 설계 및 운용은 앞서 나열한 전기차의 특성들과 직접적인 관련이 있기 때문에 이를 중심으로 실제 장점들을 평가하고, 개선할 필요가 있다. 우선 전기차의 주행에 사용되는 전기의 생산, 송전, 변환 과정들을 고려하면 궁극적인 연비 및 환경에의 영향은 알려진 것처럼만큼 크지는 않다. 전기차에서 적극적으로 활용되는 회생제동은 운동에너지를 바로 전기 에너지로 바꾸는 것으로 전기의 생산, 송전, 변환 과정으로부터 오는 에너지 손실을 줄여주며, 전기차의 에너지 효율을 높이는데 핵심적인 역할을 한다. 본 논문에서 제안하는 하이브리드 에너지 저장장치의 사용은 회생 제동의 효율을 높여 전기차의 실제 효율을 높이는데 기여한다. 또한 전기차 가격의 50%에 달하는 대용량 배터리의 높은 가격과 8~10년에 불과한짧은 배터리 수명으로 인한 감가상각 또한 전기차의 실질적인 연비를 낮추는 요인이된다. 하이브리드 에너지 저장장치의 사용과 시스템 수준의 에너지 관리 기법은 전기차 에너지 저장장치의 효율과 수명을 개선함으로써 실질적인 연비를 높이는데도 기여한다.

본 논문에서는 전기차를 위한 하이브리드 에너지 저장장치의 설계와 운용에 관련한 여러 문제를 고려하며 에너지 효율의 극대화와 운용비용의 최소화를 꾀한다. 전기차를 위한 하이브리드 에너지 저장장치를 고려한 기존의 연구들은 에너지 효율을 최대화하기 위한 체계적인 알고리즘을 제시하기 보다는, 경험적이고 발견적인 알고리즘에 의존해왔다. 본 논문에서는 전기차 전력 시스템 구성요소들의 모델링과 체계적인 최적화를 통해

회생제동의 에너지 효율을 최대화 하였다. 슈퍼캐패시터와 배터리의 효율 모델 및 제동 프로파일을 고려하여 각 저장장치로의 충전전력을 배분하면 에너지 효율을 높일 수 있다. 전기차의 에너지 효율을 높이기 위해서는 다수의 가속 및 감속을 포함하는 긴 시간 동안의 에너지 관리에 대한 고려도 필요하다. 본 논문에서는 운전 상황의 예측을 통해 다음 감속 및 가속에 대비하여 미리 슈퍼캐패시터의 충전량을 조절함으로써 에너지 효율을 높이는 기법을 제시한다. 또한 태양전지를 구비한 가정집의 전기차 충전 요금 최소화를 위한 기법을 제시한다. 태양전지에서 생산되는 전력은 전기차의 환경적인 장점을 최대화할 수 있을 뿐만 아니라 사용자의 전기 요금을 줄이는데도 효과적이다. 태양전지에서 생산되는 전력과 값이 싼 심야 시간의 전기를 활용하여 전기차를 충전하는 기법을 제시함으로써 전기차의 운용 비용을 최소화한다. 마지막으로 하이브리드 에너지 저장장치를 구비한 전기차를 실제 구현함으로써 본 논문에서 제시된 기법들의 효용성을 실증한다.

주요어: 전기차, 배터리-슈퍼캐패시터 하이브리드, 회생제동, 충전/방전 비대칭성, 전력망에 연결된 태양전지 시스템, 전기요금 최소화

학번: 2008-20881

감사의 글

대학원에 들어와 학위과정을 밟는 짧지 않는 시간 동안 도움을 준 많은 분들께 감사를 표합니다. 때로는 힘들고 어려운 시간기도 했지만 많은 것들을 배울 수 있었고, 제 인생에 다시 없을 경험인 학위과정을 밟으면서 이 분들이 아니었다면 본 논문도 없었을 것입니다. 먼저 6년이라는 기간 동안 많은 관심과 격려로 열정적으로 지도해주신 장래혁 교수님께 감사의 말씀을 전해드립니다. 바쁘신 와중에도 학위 논문을 지도해주신 하순회 교수님, 최기영 교수님, Samarjit Chakraborty 교수님, Massimo Poncino 교수님께도 감사드립니다.

앞서 훌륭한 연구를 수행하여 이 연구의 기반을 쌓아주신, 또한 많은 조언을 주고, 때로는 따끔한 질타의 말도 해주며 도움을 주신 영진형, 경수형, 동화형, 재현형, 지훈형, 재민형에게도 많은 감사를 드립니다. 또한 오랜 시간을 함께하며 연구뿐만 아니라 여러가지 측면에서 의지가 되었던 영현이에게도 고마움을 전합니다. 힘이 되어준 주은이, 재암형, 병호, 현진이, 주연이, 영신이, 기태씨, 범규 등 연구실 후배들에게도 감사의 말을 전합니다.

항상 저를 위해주시는 아버지, 어머니, 이쁜 동생과 그리고 항상 격려의 말씀을 주시는 장언어른 장모님께도 감사의 말씀을 전합니다. 때로는 힘들기도 했던 대학원 기간 내내 응원해준 지금은 사랑하는 아내가 된 효은이와, 많이 놀아주지도 못하고 잘해주지 못한 딸

가빈이에게도 미안한 마음과 감사한 마음을 함께 전해드립니다.

이제 오랜 시간 생활해온 연구실을 뒤로 하고 새로운 길을 걸으려 합니다. 항상 성실한 연구자의 자세를 잊지 않으며 보람찬 인생을 살 수 있도록 하겠습니다.